Landslide Assessment and Mapping Using Frequency Ratio and Analytical Hierarchy Process at Maze Catchment, Gamo Zone, Southern Ethiopia

Obse Kebeba Debele

A Thesis Submitted to the Department of Applied Geology

School of Applied Natural Science

Presented in Partial Fulfillment of the Requirement for the Degree of Master's in Applied Geology (Specialization in Engineering Geology)

Office of Graduate Studies

Adama Science and Technology University

February, 2024

Adama, Ethiopia

Landslide Assessment and Mapping Using Frequency Ratio and Analytical Hierarchy Process at Maze Catchment, Gamo Zone, Southern Ethiopia

Obse Kebeba Debele

Main advisor: Leulalem Shano (PhD)

Co-advisor:Yadeta Chemdesa (PhD)

A Thesis Submitted to the Department of Applied Geology,

School of Applied Natural Science

Presented in Partial Fulfillment of the Requirement for the Degree of Master's in Applied Geology (Specialization in Engineering Geology)

Office of Graduate Studies

Adama Science and Technology University

February, 2024

Adama, Ethiopia

DECLARATION

I hereby declare that this Master Thesis entitled "Landslide Assessment and Mapping Using Frequency Ratio and Analytical Hierarchy Process at Maze Catchment, Gamo Zone, Southern Ethiopia" is my original work. That is, it has not been submitted for the award of any academic degree, diploma or certificate in any other university. All sources of materials that are used for this thesis have been duly acknowledged through citation.

Obse Kebeba Debele	________________________	________________
Name of the student	Signature	Date

RECOMMENDATION

We, the advisors of this thesis, hereby certify that we have read the revised version of the thesis entitled "Landslide Assessment and Mapping Using Frequency Ratio and Analytical Hierarchy Process at Maze Catchment, Gamo Zone, Southern Ethiopia" prepared under my guidance by Obse Kebeba Debele submitted in partial fulfillment of the requirements for the degree of Masters of Science in applied geology (Specialization in Engineering Geology).

Therefore, we recommend the submission of revised version of the thesis to the department following the applicable procedures.

Leulalem Shano (PhD) ____________________ ____________________

Major Advisor Signature Date

Yadeta Chemdesa (PhD) ____________________ ________________

Co-advisor Signature Date

APPROVAL PAGE

We, the advisors of the thesis entitled "Landslide Assessment and Mapping Using Frequency Ratio and Analytical Hierarchy Process at Maze Catchment, Gamo Zone, Southern Ethiopia" and developed by Obse Kebeba Debele, hereby certify that the recommendations and suggestions made by the board of examiners are appropriately incorporated into the final version of the thesis.

Leulalem Shano (PhD)	____________________	____________________
Major Advisor	Signature	Date
Yadeta Chemdesa (PhD)	____________________	____________________
Co-advisor	Signature	Date

We, the undersigned, members of the Board of Examiners of the thesis by Obse Kebeba Debele have read and evaluated the thesis entitled "Landslide Assessment and Mapping Using Frequency Ratio and Analytical Hierarchy Process at Maze Catchment, Gamo Zone, Southern Ethiopia" and examined the candidate during open defense. This is, therefore, to certify that the thesis is accepted for partial fulfillment of the requirement of the degree of Master of Science in Applied Geology (Specialization in Engineering Geology)

____________________	____________________	____________________
Chairperson	Signature	Date
____________________	____________________	____________________
Internal Examiner	Signature	Date
____________________	____________________	____________________
External Examiner	Signature	Date

Final approval and acceptance of the thesis is contingent upon submission of its final copy to the Office of Postgraduate Studies (OPGS) through the Department Graduate Council (DGC) and School Graduate Committee (SGC).

____________________	____________________	____________________
Department Head	Signature	Date
____________________	____________________	____________________
School Dean	Signature	Date
____________________	____________________	____________________
Office of Postgraduate Studies, Dean	Signature	Date

ACKNOWLEGMENTS

I would like to begin by expressing my deepest gratitude to the Almighty God, whose divine guidance and blessings have sustained me throughout these studies. I would like to express my sincere gratitude to my advisor, Dr. Leulalem Shano, and co-advisor, Dr. Yadeta Chemdesa, for their invaluable guidance and support throughout this thesis.

I would also like to extend my sincere appreciation to Wollega University, which has provided me with financial support and resources to conduct my research.

I would like to thank the Geological Survey of Ethiopia for their support in providing the geological map and the Ethiopian Meteorological Agency for their support in providing the metrological data needed for my thesis work. I appreciate the assistance of the field laborers in collecting data during the field survey.

Furthermore, I want to recognize my friends and family members who have provided emotional support throughout this journey. Their encouragement and unwavering belief in me have been immensely meaningful, and I deeply appreciate their presence in my life.

TABLE OF CONTENTS

LIST OF FIGURES

Figure Pages

LIST OF TABLES

Table Pages

LIST OF PLATE

Plate page

LIST OF ABBREVIATIONS AND ACRONYMS

AHP	Analytic Hierarchy Process
AUC	Area Under Curve
Arc GIS	Aeronautical Reconnaissance Coverage Geographic Information System
DEM	Digital Elevation Model
EARS	East Africa Rift System
FR	Frequency Ratio
GPS	Global Positioning system
USGS	United States Geological Survey
LSM	Landslide Susceptibility Maps
LSI	Landslide Susceptibility Index
LULC	Land Use land Cover
MER	Main Ethiopian Rift
NDVI	Normalized Difference Vegetation Index
SNNPR	South Nation Nationality People Region
ROC	Receiver Operating Curve

ABSTRACT

Landslides are one of the natural threats that cause loss of life and destruction of property in Ethiopia. This study was conducted in the Maze watershed in the Gamo zone, southern Ethiopia. The objective of this study was to assess and map the landslide susceptibility of the area using frequency ratio and analytic hierarchy process (AHP) approaches. To achieve this objective, landslides inventory data and their causative factors were identified. About 793 landslide polygons were collected by using remote sensing and field observations. These landslide inventory datasets were classified into two datasets, landslide training dataset (70%) for mapping landslide susceptibility and validation landslide dataset (30%) for validating landslide susceptibility maps. Ten landslide causative factors were selected for this study including slope, aspect, curvature, lithology, land use/land cover, normalized vegetation index and distance to fault, distance to river, and distance to road. The landslide susceptibility map was produced by superimposing the weights of all landslides causative factors using the raster calculator in the spatial analysis tools in Arc GIS. The final landslide susceptibility map is reclassified into susceptibility classes of "very low," "low," "moderate," "high," and "very high" using both frequency ratio and analytical hierarchy process approaches. The results of the landslide susceptibility map created using the frequency ratio approach show that the very low, low, medium, high, and very high susceptibility classes account for 25%, 20%, 18%, 18%, and 19% of the area, respectively. The landslide susceptibility map created by the analytical hierarchical process approach shows that the very low, low, medium, high, and very high susceptibility classes cover 3%, 7%, 26%, 36%, and 28% of the area, respectively. Both susceptibility maps were validated using the area under the receiver operating characteristic curve. The AUC results for the frequency ratio and analytical hierarchy process approaches were 0.873 and 0.87 for success rates, respectively, and 0.81 and 0.80 for prediction rates, respectively. Therefore, the landslide susceptibility map using the validation dataset provided acceptable results. These maps will play an important role in land use planning efforts.

Key word: Analytical Hierarchy Process, Causative Factors, Frequency Ratio, GIS, Landslide, Susceptibility Maps

1. INTRODUCTION

1.1 Background

Earth being dynamic, the surface of the earth is always under change due to various geo-processes causing natural hazards and threat to mankind worldwide (Firomsa and Abay, 2019). Landslides are one of the destructive natural hazards that commonly lead to serious problems, especially in hilly and mountainous regions (Berhane and Tadesse, 2021). Ethiopia is one of the mountainous countries which are characterized by a steep slope, deep gorge; frequent fault escarpment, highly weathered rock, and intensive and prolonged rainfall (Wubalem, 2021). All those conditions are favorable for the occurrence of slope movements after rainy seasons in most parts of the country as (Woldearegay, 2013).

Factors that cause these landslides include unfavorable geological conditions, heavy rainfall, seismic activity, and human factors such as deforestation, urbanization, uncontrolled agricultural activities, construction, etc. (Anis et al., 2019).

In order to minimize this landslide disaster, different scientists conducted different levels of research in different landslide-affected countries (Beza, 2021; Addis, 2023). With the development of more advanced qualitative and quantitative methods and GIS data processing techniques, many studies can be conducted effectively, and as a result, landslide susceptibility, hazard, and risk assessment have attracted the attention of many researchers (Pham et al., 2015).

Landslide activity in Ethiopia mainly occurs in the north, northwestern, central, southwestern, and rift valleys due to the presence of complex geomorphological, hydrological, geological, active geodynamic processes and unplanned land use practices (Woldearegay, 2013).

The current study area is found in Maze catchment, Gamo zone, Southern Ethiopia. This area is highly susceptible to landslide problems with the occurrence of many active landslides in the last few decades which extensively damaged different infrastructures and farmlands in which the magnitude of the problem is alarming and the vulnerability of the people's lives and property from landslides needs special attention and so far, the area has not been studied before in a greater level of detail.

Anthropogenic activities have been increasing in the study area, resulting in the instability of natural slopes. In addition to this landslide occurrence is very frequent in the study area due to the area found within the part of Ethiopian highlands and therefore, there is a need for the preparation of a landslide susceptibility map for the region which can be used by planners and engineers.

1.2 Statement of the problem

Landslide is the most frequently occurring geo-hazard in mountainous regions of the world. It affects human lives, infrastructure, landscapes, and human property as well as their day-to-day activities. In the current study area which is found in the Gamo Zone of southern Ethiopia, recurrent landslide hazards have occurred. To minimize this landslide hazard on human life and their properties, landslide assessment and mapping is an important Step for environmental planning. Identifying the causative factors will help to decipher different types of slope failure, failure mechanisms and prepare the landslide susceptibility maps.

1.3 Research Question

- How can the temporal and spatial distribution of landslides be effectively represented in the inventory map?
- How does the relative influence of different causative factors vary across different spatial scales and landslide types?
- How do different types of landslides relate to specific failure mechanisms and causative factors?
- How can the spatial and temporal variability of these relationships be incorporated into landslide and assessments?
- How can the cost-effectiveness, environmental impact, and social acceptability of different remedial measures be evaluated?

1.4 Objectives

1.4.1 General objective

The main objective of this study is to assess and map the landslide susceptibility of the area using frequency ratio and analytical hierarchy process approaches.

1.4.2 Specific objectives

- To prepare a landslide inventory map.
- To identify different causative factors and characterize their influencing classes.
- To identify the mechanisms and types of failure.
- To characterize the relationships between landslides and the causative factors.
- To give the recommendation for remedial measures.

1.5 Significance of the study

Land sliding is a worldwide problem that probably results in thousands of deaths and tens of billions of dollars of damage each year, these landslides which claimed many casualties have also affected much of the farmlands and damaged the economy of the poor farmers. This led to considerable concern among the local Authorities as well as the population about the stability of the slopes in the area much of this loss would be avoidable if the problems were recognized early. This work is very important to make awareness to the local people and decision-makers. In terms of proper land use planning, various engineering work designs and civil protection - programs for various future projects.

1.6 Limitation

Notable limitation in this study was the absence of important causative factor maps, ideally at a scale of 1:50,000. Specifically, the unavailability of key maps of the lithological map. Additionally, the discontinuous record of rainfall stations from the national metrological agency of Ethiopia data introduced further constraints in this study to mapping triggering causative factor.

1.7 Organization of the thesis

The whole thesis is divided into five chapters. The first chapter lays the background of the study providing a general introduction to the research work including the statement of the problem, research questions and objectives, the significance and limitations of the study were also highlighted. The second chapter covers a literature review and presents the relevant work that has been done by many other scholars. In the third chapter, information about the chosen study area is given and how the several data layer maps are generated, also outlining the methodology of carrying out the task and the data sources utilized. Fourth chapter presents the findings of this research work and a detailed discussion of the results obtained. Finally, in the fifth chapter, a conclusion is drawn based on the results obtained and recommendations are generated for the possibilities of future researchers.

2. LITERATUREREVIEW

2.1 Landslides

Landslides are the down slope movement of rock, debris, or earth (Addis, 2022). This term encompasses various types of mass movements on slopes, including rock falls, topples, and debris flows (Varnes, 1984). Landslides occur when the weight of the slope material exceeds the shear resistance of the soil. The driving force behind landslides is gravity, which pulls everything towards the Earth's center. Consequently, materials on slopes are more susceptible to landslides than those on flat areas (Nelson, 2010).

2.2 Types of landslides

There are many ways to categorize landslides, but some of the most common types based on movement and material include:

Falls: sudden downward movement of rock or debris, often along cliffs or steep slopes (Highland and Bobrowsky, 2008).Detachment of elevated rock masses from cliffs or slopes, usually along existing cracks or weaknesses (Collins and Stock, 2016; Matasci et al., 2018).In this type of movement, the detached materials move by bouncing, falling or rolling (Hungr et al., 2014) (Figure 2.1). In such, type of failure there is no interaction between one failure and the next failure and it is fast down ward movement of slope material.

Topples: Unlike the rapid tumbling of rock falls, this type of landslide involves the gradual tilting and outward movement of large rock blocks as they rotate around a fixed point near the slope's base (Figure 2.1). Destabilization of the rock mass can occur through the infiltration of gravity, ice, or water into existing cracks and weak zones. The pace of this movement can vary dramatically, from explosively fast to almost imperceptibly slow (Highland and Bobrowsky, 2008).

Slides: downward sliding of a mass of rock or soil along a distinct surface. This can be further categorized as: Rotational slides**:** The sliding mass rotates about a curved surface and Translational slides**:** The sliding mass moves along a relatively planar surface.

In translational slides, the material moves mainly downhill along a flat or slightly inclined surface, with minimal rotation or tilting back towards the slope (Figure 2.1). This type of landslide exhibits straightforward downward movement with minimal twisting or backward motion (USGS, 2004).

Rotational slides: a spoon-shaped rupture surface curving upwards (Varnes, 1978) (Figure 2.1); this landslide type involves a rotating movement around an axis parallel to the ground and across the slide's width. Unlike translational slides, rotational slides lack major tilting or backward movement. The driving force is often the slope materials own weight exceeding its internal strength (USGS, 2004).Both rotational and translational slides, primarily affecting loose and un compacted soils, exhibit a wide range of movement speeds, from barely perceptible creeping to fast-paced slumps. While slower slides typically pose little threat to life, they can cause significant structural damage (Highland and Bobrowsky, 2008).

Lateral spread: Unlike most landslides, lateral spreads occur on surprisingly gentle slopes or even flat terrain (Figure 2.1). Instead of tumbling downhill, the ground stretches and fractures due to a phenomenon called liquefaction**.** This happens when loose, sandy, or silty sediments become saturated with water and essentially turn into liquid. This "liquid landslide" then spreads laterally, often causing significant damage to shallow foundations of infrastructure like pipelines, utilities, bridges, and roads (Highland and Bobrowsky, 2008).

Flows: Landslides classified by flow type fall into four main categories, each defined by its material composition and movement speed (Figures 2.1):

Debris flow: Dominated by water-saturated, fine-grained materials, these fast-moving landslides rush down slope, leaving a basin-shaped depression (USGS, 2004).

Debris avalanche: Similar to debris flows but involving larger rock fragments and debris**,** these high-speed movements often follow steep channels.

Creep: The slowest type involves the gradual, imperceptible downhill movement of soil and rock over time.

Earth flow: A slow-moving flow of saturated, unconsolidated soil forms a tongue-shaped mass.

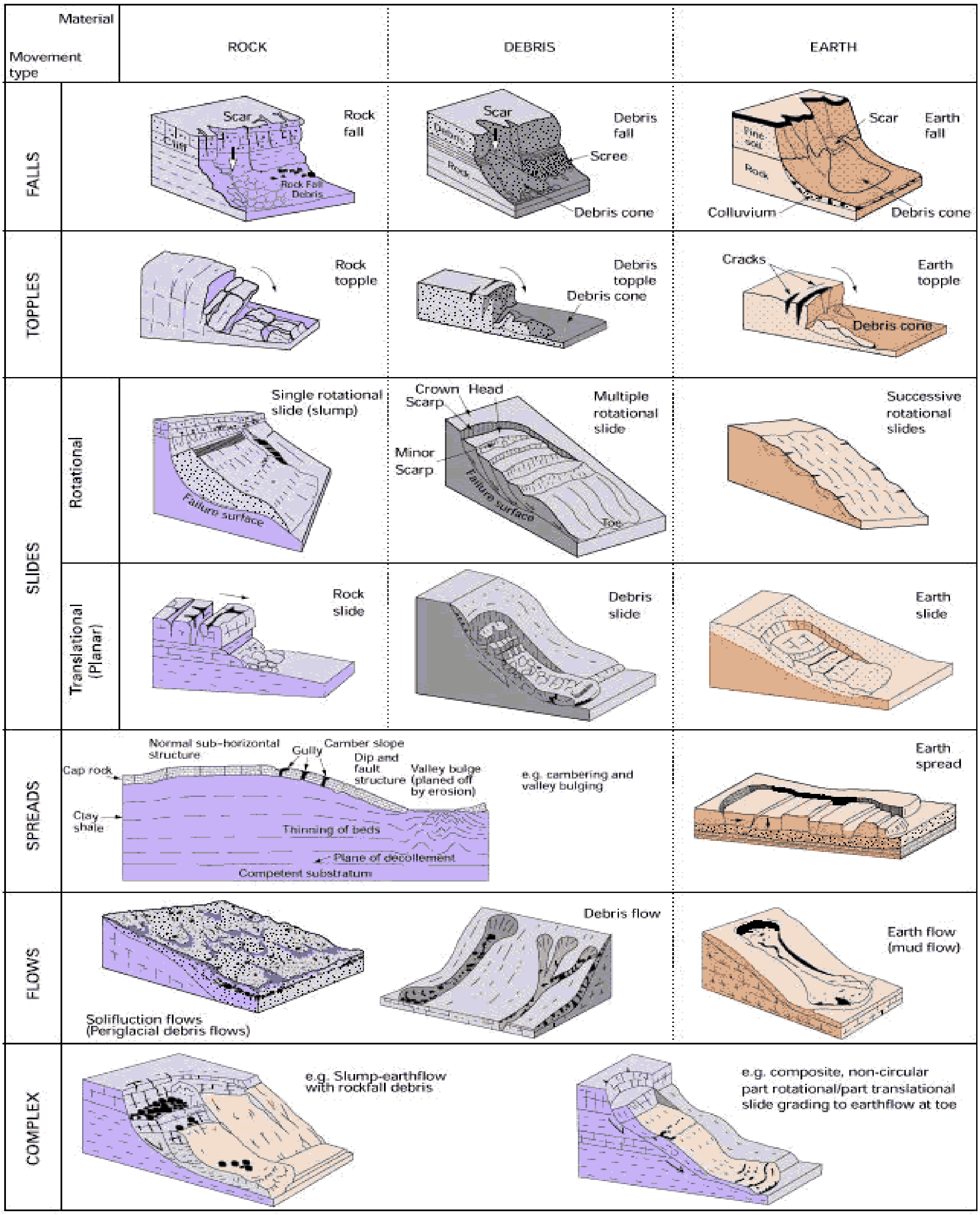

Figure 2.1 Classification of type of landslides (modified after Varnes (1978))

2.3. Landslide Inventory

Landslide inventories are crucial for mathematical modeling and validating final outputs. They contain information about landslide locations, areas, activity, and dates (Guzzetti et al., 2012). The complexity of landslide inventories varies depending on the study's requirements. The landslide inventory map rules supremely as the most crucial data layer for understanding and predicting future landslides. It carefully documents past occurrences, pinpointing locations, types, activity status, date (if known), and even damage caused (Corominas and Mavrouli, 2011). This detailed record serves as the bedrock for quantitative and qualitative analyses of landslide susceptibility, hazards, and risks. Landslide inventories are the rudimentary yet powerful chronicles of past events, forming the foundation for the adage "past is the key to the future" in landslide studies (Michael and Samanta, 2016). By meticulously recording locations, types, and dates of landslides, these maps provide the cornerstone information for both quantitative and qualitative risk assessments, paving the way for effective mitigation strategies. They are compiled from existing literature, Google Earth, and field visits by using handled GPS (Addis, 2023).

2.4 Causative factors of landslides

Landslide susceptibility maps are based on the complex relationship between landslide events and their triggering factor (Shano et al., 2021). The factors considered for landslide susceptibility assessment are chosen based on literature reviews and thorough field observations. In landslide susceptibility mapping, there is no established rule for selecting which factors to include; rather, the selection depends on the area's characteristics and data availability (Ayalew and Yamagishi, 2005).

2.4.1 Geological Factor

2.4.1.1 Lithology

Lithology encompasses the composition, fabric, texture, and other characteristics that influence the physical or chemical behavior of rocks and engineering soils. The probability of landslides is higher when rock formations are loose and fragile. Different rock types, or lithologies, exhibit varying compositions and structures, which contribute to their material strength. Kanungo et al. (2009) noted that stronger rocks offer greater resistance to driving forces compared to weaker rocks, making them less susceptible to landslides.

2.4.1.2 Structures

Geological structures significantly impact slope stability conditions. Marden et al. (1992) elaborated on the influence of geological structures on slope stability, stating that down slope dipping planes separating rocks of varying competence or alteration, along with joints and fractures aligned in the same direction, can hinder vertical infiltration and root penetration, while also serving as potential failure planes. Therefore, as evidenced by various studies, the influence of rock structures (bedding planes, folds, joints, and faults) plays a crucial role in the stability of natural hill slopes.

2.4.2 Aspect

Aspect, defined as the direction of the steepest slope inclination (Xu et al., 2012), plays a crucial role in landslide initiation through its influence on moisture retention and vegetation cover (Raghuvanshi et al., 2015). This orientation, typically expressed in degrees ranging from 0° to 360° (Mersha and Meten, 2020), can significantly impact a slope's vulnerability to landslides. According to Huang et al. (2015), aspect, the direction a slope faces, significantly influences landslide occurrence by controlling the slope's exposure to sunlight, cold and hot winds, and precipitation.

2.4.3 Slope

Slope angle, the steepness of a slope, is a crucial factor in landslide occurrence, as it influences the concentration of moisture and pore pressure within the slope material (Ayalew and Yamagishi, 2005). As the slope angle increases, the parallel component of gravity increases, while the perpendicular component decreases, making steeper slopes more susceptible to failure (Huang et al., 2015). Slope angle also plays a role in regional hydraulic continuity, influencing the movement of water across larger areas. In the study, the slope gradient was derived from digital elevation model (DEM) data with a spatial resolution of 30 meters by 30 meters.

2.4.4 Curvature

Curvature, a measure of how slope inclination changes in a specific direction, is influenced by both hydraulic conditions and gravity. It can manifest as convex, concave, or flat terrain. Concave slope curvature promotes groundwater accumulation, which can destabilize slopes. Conversely, convex slope curvature facilitates erosion, which can also contribute to slope instability (Riaz et al., 2018; Wubalem, 2021).

2.4.5 Distance from Stream

Distance from streams is a crucial factor in determining landslide susceptibility, particularly when streams undercut slope bases (Che et al., 2011). Rivers with extensive drainage networks pose a greater landslide risk due to their ability to erode slope bases and saturate slope-forming materials (Necdet, 2011).Landslide susceptibility was positively correlated with decreased distance from streams (Celek, 2019).

2.4.6 Distance from Lineament

Lineaments are linear features on the Earth's surface that represent zones of weakness or fracturing in the underlying rock or soil (Michael and Samanta 2016). They can be caused by a variety of geological processes, such as faulting, folding, or erosion. Lineaments can significantly affect the stability of slopes by influencing the permeability of the surface material, which in turn affects the flow of water and other fluids (Michael and Samanta 2016).According to Pradhan and Lee (2007) and Ilek (2019), the potential of a landslide increases as the distance from lineaments decreases. Lineaments of the study area can be prepared from Google Earth image interpretations and field surveys.

2.4.7 Land Use and Land Cover (LULC)

Land use and land cover (LULC) changes are widely acknowledged as one of the most significant factors influencing the occurrence of rainfall-triggered landslides globally (Mersha and Meten, 2020). Human activities such as deforestation, overgrazing, intensive farming, and cultivation on steep slopes can alter LULC patterns, leading to slope instability and increased landslide risk (Glade, 2003). Barren slopes, devoid of vegetation cover, are particularly susceptible to landslides due to the absence of plant roots that help bind soil particles together and reduce erosion. Vegetation also intercepts rainfall, decreasing the amount of water that infiltrates the soil and contributing to slope instability (Gomes et al., 2005). According Prandini et al. (1977) and Greenway (1987), vegetation with deep and extensive root systems positively impacts shallow debris and earth slides by enhancing soil strength through root network reinforcement and buttressing slope masses via root anchorage to the underlying bedrock.

2.4.8 Normalized Differentiation Vegetarian Index (NDVI)

The vegetation index is also considered an influencing factor in landslide susceptibility assessment studies (Tseng et al., 2015). NDVI was used in this study to reflect the vegetation density. In general, the value of NDVI ranged from -1 to 1; the higher the value of NDVI the denser the vegetation covers.

The Normalized Difference Vegetation Index (NDVI) conditioning factor was calculated from Sentinel-2 satellite imagery with a spatial resolution of 10 meters using Equation (1):

$$NDVI = (IR - R) / (IR + R) \tag{1}$$

Where, IR is the reflectance in the infrared band and R is the reflectance in the red band

2.4.9 Triggering factors

Information related to triggering factors generally has more temporal than spatial importance, except when dealing with large areas on a small mapping scale. This type of data is related to rainfall, temperature and earthquake records over sufficiently large time periods, and the assessment of magnitude-frequency relations. Rainfall and temperature data are measured in individual meteorological stations (Corominas and Mavrouli, 2023).Human activities such as the construction of roads cutting slopes and clearing of land can be triggering factors of landslide (Sideng, et al., 2018). But in this research rainfall data is the most triggering factor of landslide over the study area.

2.4.9.1 Rainfall

Precipitation affects slope stability in many ways. First, precipitation affects rock formations hence the likelihood of slope failure. Secondly, precipitation increases the amount of water in surface soils which can increase the likelihood of landslide events. Precipitation increases the saturation level of surface soils, which increases pore water pressure in the voids between soil particles. This increase in pore water pressure decreases the friction and cohesion between soil particles and may lead to shallow seated landslides and debris flows (Musinguzi and Asiimwe, 2014).

2.5 Landslide Susceptibility Mapping Techniques

Landslides pose a major threat in various regions globally, necessitating swift methods for assessing slope stability. To identify areas with varying landslide susceptibility levels, several analysis techniques exist (Anbalabgan, 1992). These methods can be categorized as expert-based (qualitative), statistical, or deterministic (quantitative) approaches (Leroi, 1997; Fall et al., 2006).

2.5.1 Qualitative evaluation technique

This technique is a qualitative approach classified into two types: inventory mapping and heuristic (geomorphic) analysis (Fall et al., 2006). Inventory mapping identifies past landslide locations and records their details like position, date of failure, size, trigger, frequency, and type (Dai and Lee, 2001; Fall et al., 2006) and depicts past landslides on maps as polygons or points (Kanungo et al., 2009). This method shows areas susceptible based on past occurrences but not the degree of future risk (Mersha and Meten, 2020) and provides valuable data for other susceptibility analysis methods (Dai and Lee, 2002; Mersha and Meten, 2020).

The heuristic approach relies heavily on expert experience to assess landslide risk. Geoscientists analyze various maps of factors like slope angle, soil type, and land use, assigning numerical ratings based on their knowledge and past observations of how these factors influence slope stability (Dai and Lee, 2002; Anbalagan, 1992). While subjective, this method is praised for its simplicity and ability to leverage existing field data enriched by expert insights (Fall et al., 2006; Raghuvanshi et al., 2014a; 2014b).

2.5.2 Statistical analysis technique

Statistical analysis techniques take a quantitative approach to assessing landslide risk, unlike the subjective expert-based methods. They rely on statistical models to identify the combination of factors influencing landslide susceptibility in a specific area (Carrara et al., 1992).

Statistical methods for landslide assessment come in two flavors: bivariate, focusing on two factors at a time, and multivariate, considering a broader range. While these methods offer an objective approach to evaluating risk, they face significant challenges: 1) Data acquisition: Gathering extensive data over large areas takes time and resources (Van Westen et al., 1997). Identifying the key factors influencing landslides adds complexity and cost. 2) Data dependence: The accuracy of the results hinges heavily on the quality of the data used. Inaccurate or incomplete data can lead to unreliable predictions (Van Westen et al., 1997).

2.5.2.1Bivariate statistical method

This statistical technique, called bivariate overlay analysis, pinpoints the relative importance of different factors in triggering landslides. It works by layering individual factor maps (e.g., slope angle, soil type) on top of a map of past landslides and calculating "weights" for each factor class based on its association with past landslides. A higher density of landslides within a factor class means they get a higher weight, indicating their stronger influence and combining these weighted maps to generate a final landslide susceptibility map (Aleotti and Chowdhury, 1999). This technique encompasses various statistical methods like information value, frequency ratio, and weight of evidence, all focused on developing landslide susceptibility mapping (Kanungo et al., 2009).

2.5.2.2 Multivariate statistical method

A multivariate statistical model forecasts the spatial occurrence of landslides. These powerful tools predict the likelihood of landslides across a landscape by considering the combined influence of various factors. Each factor, represented by a thematic data layer (e.g., slope, soil type, rainfall), contributes to the overall susceptibility to landslides, and the model calculates its relative importance (Ayalew and Yamagishi, 2005; Kanungo et al., 2009; Shano et al., 2020). This approach provides a more comprehensive and nuanced understanding of landslide risk across a wider area. After identifying landslide and non-landslide areas, a multivariate statistical model is used to reclassify the entire area into different hazard zones. This model considers the percentage of landslide-affected pixels in each zone to determine its overall susceptibility. Several Methods are commonly used for this reclassification, including: Logistic regression method, discriminant method including artificial intelligence methods, artificial neural network method, support vector machines, probabilistic approach and deterministic approach (Shano et al., 2020).

2.5.3 Deterministic approach

The deterministic approach is a quantitative method for assessing landslide risk, offering definite predictions within a factor of safety (Raghuvanshi et al., 2014a). Unlike the probabilistic approach, which gives a range of possibilities, the deterministic approach provides concrete results directly applicable to engineering designs (Fall et al., 2006).

The deterministic approach works best for small to medium-sized landslides, where large or medium-scale mapping allows for gathering the detailed geotechnical and hydrological data it requires (Raghuvanshi et al., 2014a; Van Westen et al., 2006). At larger scales, data collection becomes more challenging, limiting its applicability.

2.6 Selection criteria

The selection of an appropriate technique for landslide susceptibility and assessment depends on several factors, including the study's objectives, the area's size, the desired mapping units, the map scale, the type and availability of data, the landslide types, the availability of resources, the evaluator's expertise, and the study area's accessibility (Guzzetti et al., 2000, 2012; Van Westen et al., 2005).

2.6.1 Analytic Hierarchy Process (AHP) Approach

The Analytic Hierarchy Process (AHP) is a decision-making tool that facilitates the decomposition of complex problems into simpler, more manageable criteria. It employs a structured approach that encompasses problem definition, goal and alternative identification, pairwise comparison matrix formulation, weight determination, and overall priority determination (Pardeshi et al., 2013; Saaty, 2008).

The AHP effectively addresses the limitations of arbitrary weight and score approaches by enabling decision-makers to derive ratio-scale priorities or weights rather than assigning them arbitrarily (Yalcin, 2007).

The Analytic Hierarchy Process (AHP) offers a hierarchical structure of criteria, allowing users to concentrate on specific criteria and sub-criteria while assigning weights (Ishizaka and Labib, 2009). However, a drawback of the AHP is the large number of pairwise comparisons required, involving comparisons of individual criteria and alternatives against each criterion. The AHP approach can be employed in either an absolute or relative measurement of the relationship between causative factors and landslides. In absolute measurement, each alternative is compared to a single ideal alternative, while in relative measurement; each alternative is compared to multiple alternatives. According to Pardeshi et al. (2013), Saaty and Vargas (2006), and Saaty (2008), the relative measurement approach is subjective and dependent on the evaluator's experience and ability to assess observations.

To make informed and structured decisions, it is essential to break down the decision process into manageable steps. The application of the Analytic Hierarchy Process (AHP) to a decision problem involves four distinct phases (Saaty, 1980; Zahedi, 1986; Saaty, 2008):

1. Problem Structuring: Establishing a hierarchical framework for the decision problem, clearly defining the decision objectives, identifying relevant criteria, and arranging them in a hierarchical manner (Abay and Barbieri, 2012).

2. Pair-wise Comparisons: Conducting pair-wise comparisons of the decision criteria was to determine their relative importance. This involves assessing the relative preference between each pair of criteria and assigning numerical values to represent these preferences (Saaty, 1980).

3. Local Weights and Consistency: Calculating local weights for each criterion based on the pair-wise comparisons and evaluating the consistency of the judgments. Ensuring consistency ensures that the decision-makers preferences are internally consistent and reliable (Saaty, 2000).

4. Weight Aggregation: Aggregating the local weights to derive the overall priority weights for each alternative or option within the decision problem. This step provides a comprehensive understanding of the relative importance of each alternative.

The consistency of the weights for relative importance assigned during the pair wise comparison was checked using the equation given below.

Table 1Random Consistency Index (RI) *(*source Saaty, 1980, 2000*)*

n	1	2	3	4	5	6	7	8	9	10	11	12	13	14	15
RI	0	0	0.58	0.9	1.12	1,24	1.32	1.41	1.45	1.49	1.51	1.53	1.56	1.57	1.59

2.6.2 Frequency Ratio Model

The frequency ratio model assumes that future landslides will occur under conditions similar to those observed in past landslide-prone areas within the study region. Due to its simplicity and ease of implementation within a GIS environment, the frequency ratio model is a widely used technique for landslide susceptibility mapping (Yalcin et al., 2007). The frequency ratio approach establishes a connection between the distribution of landslides and various factors associated with landslides, allowing for the correlation of landslide locations with these factors within the study area (Lee and Pradhan, 2007). To determine the frequency ratio, the area ratio of landslide occurrence and non-occurrence was calculated for each class or type of factor. Subsequently, an area ratio for each class or type of factor relative to the total area was determined. The larger the ratio is, the stronger is the relationship between landslide occurrence and the given factor's attribute.

2.7 Regional Geology of the Study Area

The current study area is located in Ethiopia's Southern Rift Basin; the geology of the region is characterized by Cenozoic rocks of the Tertiary and Quaternary periods and Precambrian rocks of the Archean and Proterozoic eons. Quaternary basalts form the Hamasa River (Humbo) Volcanic Field between Lake Abaya and Dimtu town. The basalt is dark gray in color, while slightly differentiated trachy basalts are light gray. The basalt is fine-grained and olivine phyric, with columnar jointing. The Quaternary lavas are faulted by a system of grabens parallel to the Bilate River.

Quaternary Alluvial deposits comprising gravels, clay sands, and silts form alluvial fans where rivers enter Lake Abaya. A large delta of the Bilate River is located on the northern shore of Lake Baya, and a large alluvial plain can be found on its western shores to the north of Arba Minch, which forms stratified layers.

The oldest volcanic rocks are the Lower Basalt, Rhyolites, and Trachyte in the region. They occurred in the southern and southeastern parts of the region, covering an area of 774 square kilometers (Katzmin, 1972). The Lower Basalt was characterized by thick, extensive lava flows that exhibit columnar jointing in some areas and intense weathering. There is considerable variation in texture among the flows of the Lower Basalt. This unit also includes minor bodies of rhyolite, ignimbrite, and olivine-plagioclase-phyric basalt (Tefera et al., 1996). pyroclastic flows of the region mainly combined with ignimbrite and stuff, lower basalt flow; stratified basalt flows with rare basaltic pyroclastics; lower trachyte flows; it contains massive trachytes along the Omo River, quartzo-field spathic gneiss, biotite, and amphibole gneiss, magmatic in part, with minor quartzo-field spathic gneiss and late-tectonic granite in the region.

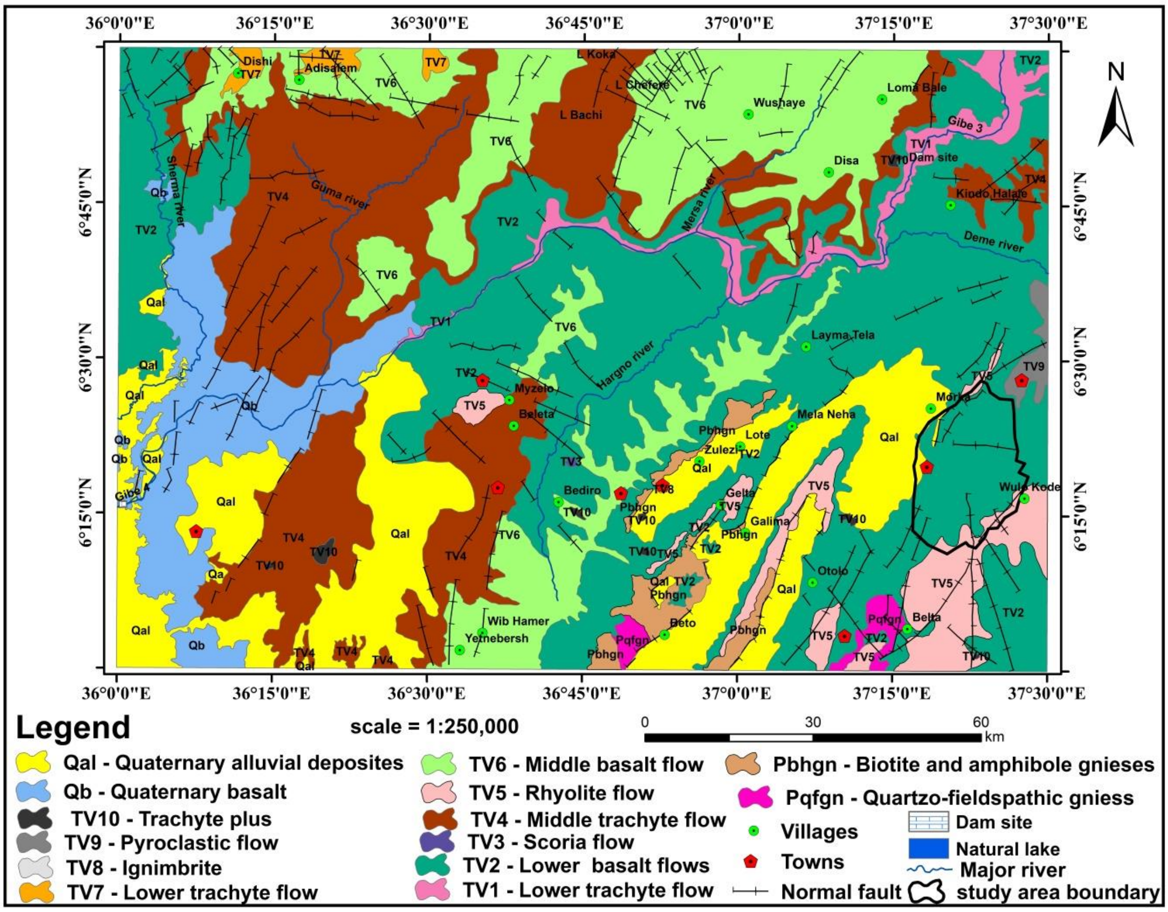

Figure 2.2 Geological map of Dime prepared by Tarekegn Dure, Abebe Misgie and Melese Tute (2017)

3. MATERIAL AND METHODS

3.1 Description of study area

The study area is located in Gamo zone South Ethiopia. It is found at distance of around 460km far from Addis Ababa capital city of Ethiopia. Geographically, located between 6°12'N and 6°28'N Latitude and between 37°16'E and 37°28'E Longitude. The elevation ranges between 1056m up to 3540m m above sea level (Figure 3.1). This area can be classified into two main physiographic regions: - plateau area and rugged terrain. The area is highly susceptible to active surface processes because of the presence of cliffs, rugged slope faces, steep scarps, deep gorges, and valleys.

The study area is vegetated, with eucalyptus, tsid, and bushes covering most ridges. Most of the study area is moderately slope to very steep sloping terrain, which are heavily used for agriculture. Teff, Sorghum, Barley, Wheat, Beans, maize, potato and ensete are the most widely grown agricultural crops.

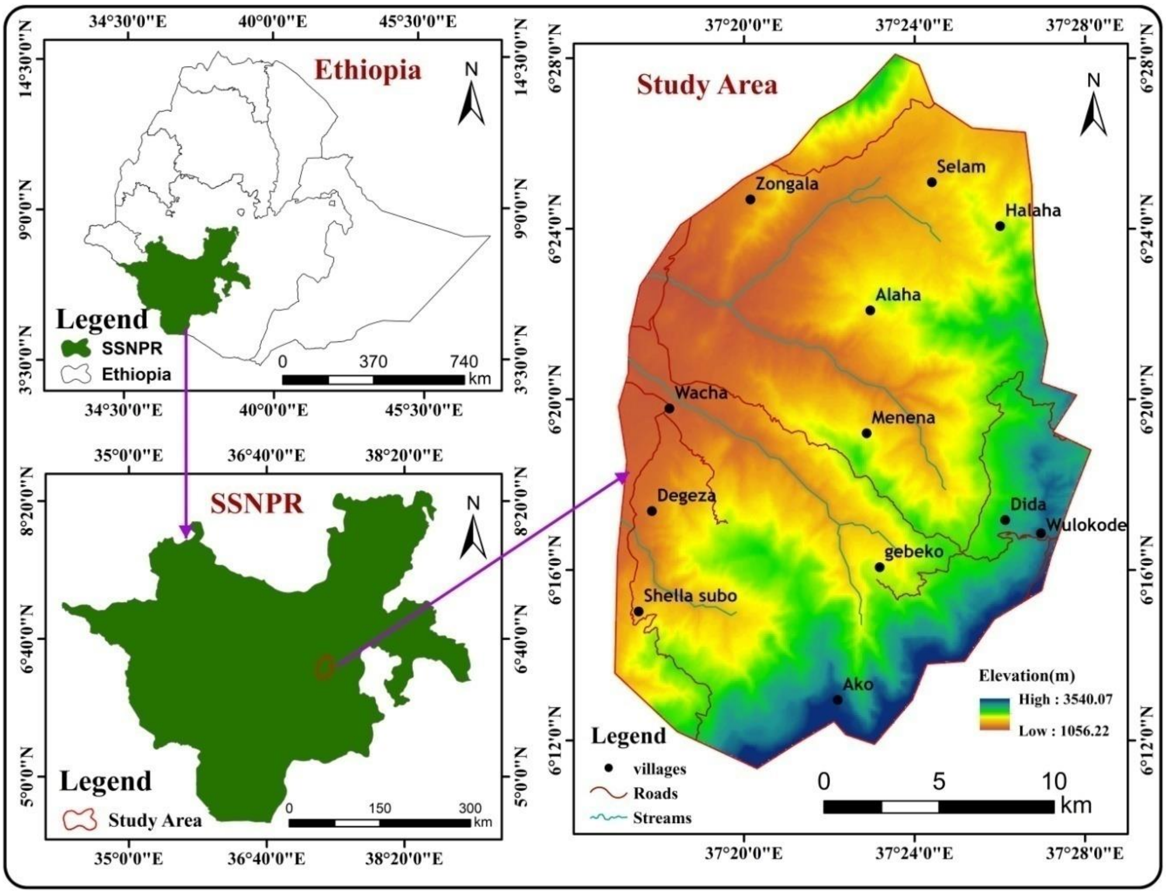

Figure 3.1 Location map of study area

3.1.1 Climate conditions

The climatic condition of the area showed that the wet season starts in May and extends up to October, and the peak wettest season occurs in July and August with a maximum monthly rainfall of 477mm and 440mm, respectively (Figure 3.2). This area receives rainfall twice a year, with heavy precipitation from June to September and light to moderate precipitation from mid-March to mid-May. The main rainy season is from June to the end of September. As indicated in Figure 3.3, the peak average annual rainfall was 3314mm and the minimum was 710mm. Appendix I, indicates the rainfall data for all stations given by the National Meteorological Agency of Ethiopia.

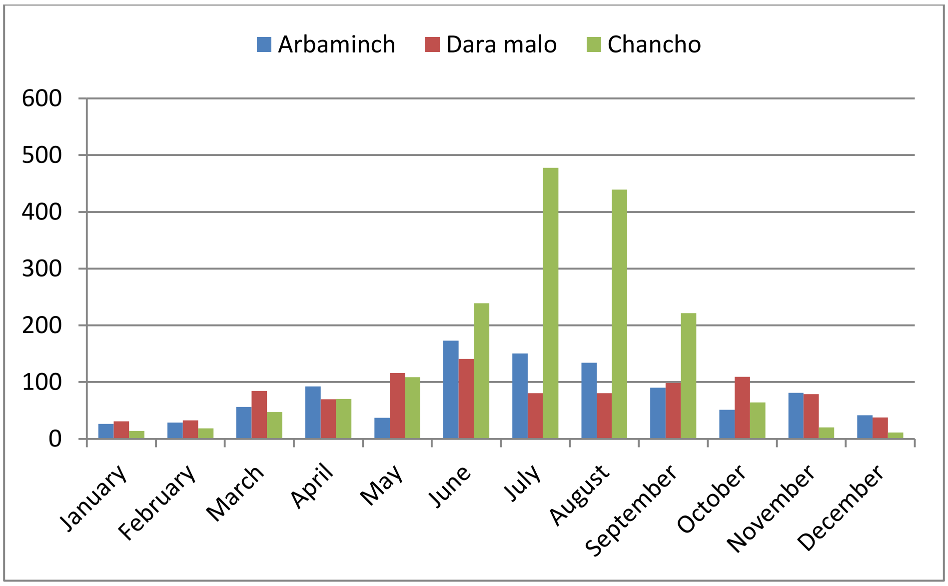

Figure 3.2 Average monthly Rainfall of the study area

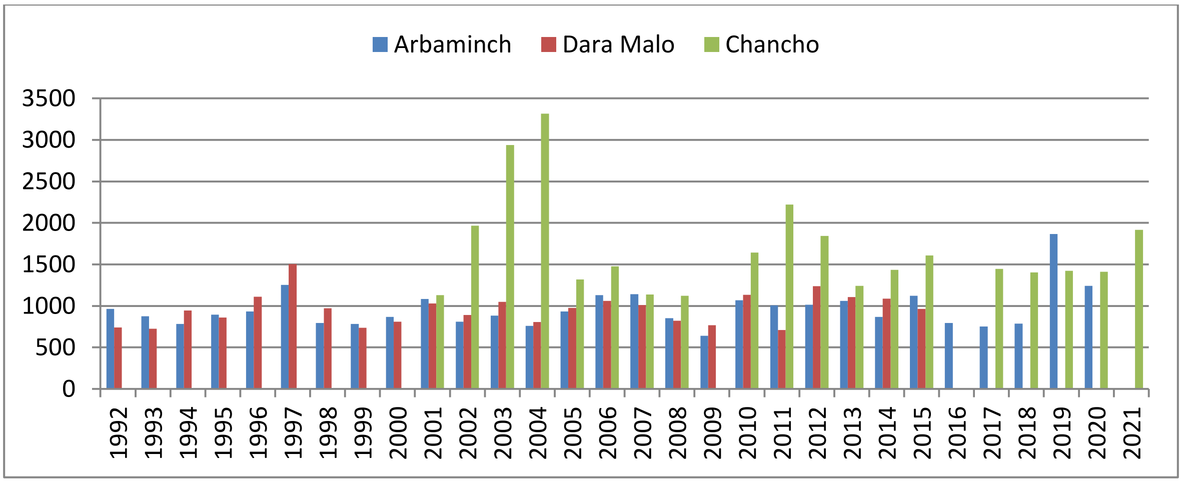

Figure 3.3 Average annual Rainfall of the study area

3.2 Materials and Software

Materials are the essential tools and resources employed to identify and address landslide-related issues. These materials play a crucial role throughout the research process, encompassing both primary and secondary data collection, evaluation, interpretation, and other aspects. The specific materials and software used in this study include the following: GPS (Global Positioning System) is a handheld device that provides accurate location data for precise mapping and identification of landslide sites. The digital camera was a tool used to capture high-quality images of landslide features and the surrounding landscape, providing visual documentation for further analysis. A compass was an instrument employed to determine the orientation of geological features and landslide deposits, aiding in the interpretation of landslide mechanics. Tape Measure was a tool used to measure various dimensions of landslide features, such as length, width, and depth, providing quantitative data for landslide characterization. Notebook: This tool was used to record detailed field observations, including descriptions of landslide features, environmental conditions, and any notable findings, providing valuable information for subsequent analysis and interpretation.

Various software were utilized for this task including Microsoft Office Word 2019 and Microsoft Office Excel 2019 version were used for data handling and report writing. Additionally, Microsoft Office Excel 2019 was used to overlay area under curve graph of success rate and predictive rate of both FR and AHP susceptible maps, and estimate pair-wise comparisons for AHP approach. For the preparation of different thematic map layouts, Arc GIS version 10.8.1 was used. Google earth pro was used to prepare landslide inventory, and lineament identification.

3.3 Methods

3.3.1 Data Collection

This is the basic data needed to achieve the objective. These data were categorized into two categories: primary and secondary data.

In order to assess accuracy of the assessment, high quality of Google earth image investigation was used. The data was used for validating the causative factor maps and landslide inventory map for the areas. Thus, Google earth pro data are primary data used.

The following tasks were completed during investigation:

- Relevant information about the locations, modes of failure, and sizes of previous landslides was gathered.
- Visual Documentation: Photographs were captured to document the geological features, topographical variations, and remnants of past landslides within the study area.
- Anthropogenic Influences: Information pertaining to human-induced activities, including excavations, slope stabilization measures, quarrying operations, and road or structure construction, was carefully noted.
- Geological Verification: The existing geological map was thoroughly reviewed and verified during the field investigation to ensure its accuracy and relevance.
- Land Use/Land Cover Analysis: The types of land use and land cover patterns were identified and validated to assess their potential influence on landslide susceptibility.
- Lineament and fault Identification: Linear features, known as lineaments, and fault were carefully mapped and analyzed, as they often represent zones of weakness that may contribute to landslide initiation.

Secondary data were collected from different institutions/organizations, including a literature review on both published and unpublished papers from different online and journal sources, regional geological map from the Geological Institute of Ethiopia and metrological data from National Meteorological Agency of Ethiopia.

3.3.2 Data Analyses Methods

For landslide susceptibility mapping, existing landslides are used to evaluate the possible areas of future landslides. The bivariate and multivariate statistical approaches are used to analyze the spatial distribution of landslides in the landslide susceptibility maps. Bivariate statistical analyses perform an individual statistical assessment of each factor in relation to landslide occurrence. Several bivariate (information value, weights of evidence, certainty factor function, and frequency ratio) approaches were developed for landslide susceptibility mapping (Pradhan, 2007). Multivariate statistical models like logistic regression method, artificial intelligence methods, artificial neural network method, support vector machines, probabilistic approach, and deterministic approach are used to forecast spatial landslide occurrence (Shano et al., 2020). For this study, frequency ratio and the analytical hierarchy process were selected; hence, frequency ratio estimation was simple and used to quantitatively assess the landslide susceptibility, and the analytical hierarchy process was also adopted for analysis to ascertain the relative importance of the criteria based on the expert responses and literature reviewed.

3.3.2.1 Landslide susceptibility mapping using frequency ratio method

The frequency ratio approach is based on the observed relationships between the distribution of landslides and each landslide-related factor to reveal the correlation between landslide location and the factors in the study area (Lee and Pradhan, 2007).

In order to evaluate the relationships between the causative factors and landslide distribution, each causative factor was reclassified, and landslides were overlaid over each factor map to determine the frequency ratio values of all the classes of each factor map (equation 3 and 4) in ArcGIS.

$$\text{Frequency Ratio (FR)} = \frac{\text{Slide Ratio}}{\text{Class Ratio}} \tag{2}$$

$$\text{Slide Ratio} = \frac{\text{Number of landslide pixel in class}}{\text{Total number of landslide pixel}} \tag{3}$$

$$\text{Class Ratio} = \frac{\text{Number of pixel in individual class}}{\text{Total number of pixel in whole class}} \tag{4}$$

The FR value represents degree of the correlation between landslides and the concerned class of the conditioning factors. So, a value of 1 means an average value. If the value is > 1, there is a high correlation, and FR < 1 means a lower correlation (Hyun et al., 2009). Then, the landslide susceptibility index (LSI) was calculated in spatial analysis tools of raster calculator by adding FR values of all causative factors as equation 5 below (Pradhan, 2006).

$$\text{LSI} = \Sigma\text{FR} = \text{FR1} + \text{FR2} +. . + \text{FRn}. \tag{5}$$

The frequency ratio values for each landslide factor were tabulated and graphically plotted in a Microsoft Excel spreadsheet based on equation 1. Then, the frequency ratio values of each factor map class were assigned in ArcGIS, and finally, the frequency ratio of all the factor maps was added to the raster calculator of the spatial analysis tools to produce the landslide susceptibility index (equation 5) and the landslide susceptibility index was reclassified in to five landslide susceptibility classes.

3.3.2.2 Landslide susceptibility mapping using the Analytical Hierarchy Process Method

It is necessary to break the decision down into steps in order to make a decision in an orderly manner and create priorities. Application of AHP to a decision problem considers four steps (Saaty, 1980; Zahedi, 1986; Saaty, 2008): (1) Structuring of the decision problem in a hierarchical approach, (2) Making pair-wise comparisons and obtaining the judgmental matrix, (3) Computing local weights and consistency of comparisons, and (4) Weights aggregations.

Step-1: Structuring of the decision problem in a hierarchical approach this step allows a complex decision to be structured into a hierarchy descending from an overall objective to various ‘criteria’, ‘sub-criteria’, and so on until the lowest level. The overall goal of the decision is represented at the top level of the hierarchy while the criteria and sub-criteria contributing to the decision are represented at the intermediate levels. Finally, the decision alternatives are positioned at the last level of the hierarchy. In this study the hierarchy of the landslide causative factors (criteria or sub-criteria) is adopted from the correlations studied by applying frequency ration model (Abay and Barbieri, 2012) besides to the field observations.

Step-2: Constructing pair-wise comparisons and obtaining the judgmental matrix once the hierarchy has been structured, the next step is to construct the pair-wise comparison matrix as proposed by Saaty (1980). The input data for problem consists of matrices of pair-wise comparisons of elements of one level that contribute to achieve the objectives of the next higher level. That is, the elements of a particular level are compared with respect to a specific element in the immediate upper level. Once the matrix is created, elements are compared pair-wise to determine their relative importance in terms of each criterion (factors) based on the scale introduced by Saaty (1980). According to this scale, the available values for the pair-wise comparisons are members of the set: {1/9, 1/8, 1/7, 1/6, 1/5, 1/4, 1/3,1/2, 1,2,3,4,5,6,7,8,9} (Table 2).

Table 2 fundamental scale of relative importance (saaty, 2008)

Intensity of Importance	Definition	Explanation
1	Equal importance	Two activities contribute equally to the objective
2	Weak importance	
3	Weak importance of one over another	Experience and judgment slightly favor one activity over another
4	Moderate	
5	Essential or strong importance	Experience and judgment strong favor one activity over another

6	Strong	
7	Very strong importance	An activity is strongly favored and it dominance demonstrated
8	Very, very strong	
9	Extreme importance	The evidence favoring one activity over another is of the highest possible order of affirmation

Step-3: Computing local weights and consistency of comparisons

The aim of this step is to find a set of priorities or local weights, which is the normalized Eigen vector of the elements of the matrix. Although different methods have been used to derive the priorities, we employed the Eigen-value technique for computing the weights under AHP, which is one of the common methods developed by Saaty (1980). The steps followed to compute the criterion weights (Eigen vector) of a reciprocal matrix involved the following operations:

(i) Summing of the values in each column of the reciprocal matrix; (ii) Divide each element in the matrix by its column total (the resulting matrix is referred to as the normalized pair wise comparison matrix and the sum of each column is 1); and (iii) Compute the average of the elements in each row of the normalized matrix, that is, divide the sum of normalized scores for each row by the number of criteria. These averages provide an estimate of the relative weights of the criteria being compared. The priority vector shows relative weights among the things that we compare. The higher the weight is the more important the criteria.

Priorities or relative weights make sense only if derived from a consistent or near consistent matrices. Thus, checking the consistency of reciprocal matrix is vital. To do that, weneed what is called Principal Eigen value (λmax) which is an important validating parameter in AHP. It is used as a reference index to screen information by calculating the Consistency Ratio (CR) (Saaty, 2000) of the estimated vector in order to validate whether the reciprocal matrix provides a completely consistent evaluation. The CR is calculated as per the following steps:

i) Calculate the eigenvector and largest Eigen value (λmax) for each matrix of order n. Principal Eigen value (λmax) is obtained from the summation of products between each element of Eigen vector and the sum of columns of the reciprocal matrix.

ii) Compute the consistency index (CI) for each matrix of order ‘n’ by the formulae:

$$CI = \frac{(\lambda\max) - n}{n - 1} \tag{6}$$

iii) Calculate the CR using the formulae:

$$CR = \frac{CI}{RI} \tag{7}$$

Where, RI is random consistency index obtained from a large number of simulation runs and varies depending upon the order of matrix (Table 1).

If the value of the consistency ratio was less than ten percent (10%), the provided weight values for each factor parameter were accepted, unless the relative importance provided was rechecked. Then, by using a weighted sum procedure in spatial analysis tools, the landslide susceptibility index AHP approach was produced as equation (8) (Komac, 2006), and it is reclassified into five susceptibility classes.

$$LSI = \sum \mathrm{Fi}w\mathrm{i} \tag{8}$$

Where, LSI is landslide susceptibility index, F is causative factors, w is normilazed weight and i is number of factors

3.3.2.3 Verification of the Landslide Susceptibility Maps

In this study, the combination of the landslide susceptibility and landslide inventory map was typically used to determine the quality of a landslide susceptibility maps. From the total landslides found, (30%) were used to test the developed maps. Both the frequency ratio and analytical heirachy process were used to investigate the landslide susceptibility.

For validation, the area under the curves (predictive and success rates) was used by using the 30% validation landslides in both landslide susceptibility maps. The success rate was estimated by comparing the training data set with the landslide susceptibility class, whereas the predictive rate was calculated by comparing the validation data set with landslide susceptibility classes by using SDM tools which downloaded and added to arctool box in GIS enviroment.

3.4 Landslide inventory data

The landslide inventory map serves as the cornerstone of landslide susceptibility assessments, providing crucial insights into the spatial distribution of past landslide occurrences. It encompasses information on the location, type, state of activity, date of occurrence (if available), and the damage caused by past landslides. This historical data is invaluable for understanding the patterns and trends of landslide occurrence, enabling the identification of potential hazard zones and the development of effective mitigation strategies (Corominas andMavrouli, 2023).

Landslide inventories adhere to the principle that "the past is the key to the future," utilizing past landslide events to inform predictions about future landslide susceptibility (Fell et al., 2008). By recording the location, date, type, size, activity, and causal factors of landslides, landslide inventories provide a comprehensive understanding of landslide dynamics and their potential impacts (Aipe and Sailesh, 2016). This knowledge is essential for developing effective land management practices and reducing landslide risk. This study digitized the landslide inventory map from Google earth image interpretation and field survey.

3.5 Data Analysis

Data analysis involved primary and secondary data sources, following these procedures:

- Landslide Inventory Polygon: The landslide inventory polygon was created by digitizing and rasterizing a Google Earth image from 2023 and field survey using ArcGIS 10.8.1.
- Causative Factor Maps: Thematic maps of landslide causative factors were created using both secondary and primary data sources within ArcGIS 10.8.1. These maps were then converted to raster format with a uniform cell size of 30 by 30 meters.
- Landslide Susceptibility Index Maps: Landslide susceptibility index maps were calculated for the frequency ratio using the Raster Calculator tool in ArcGIS and for Analytic Hierarchy Process susceptibility index was calculated in weighed sum of spatial analysis tools in ArcGIS 10.8.1.
- Landslide Susceptibility Classes: Five landslide susceptibility classes were defined for both frequency ratio and Analytic Hierarchy Process models: very low, low, moderate, high, and very high.
- Validation: The landslide susceptibility maps were validated against a validation landslide inventory map, comparing the predictive and success rates using the AUC of ROC values.

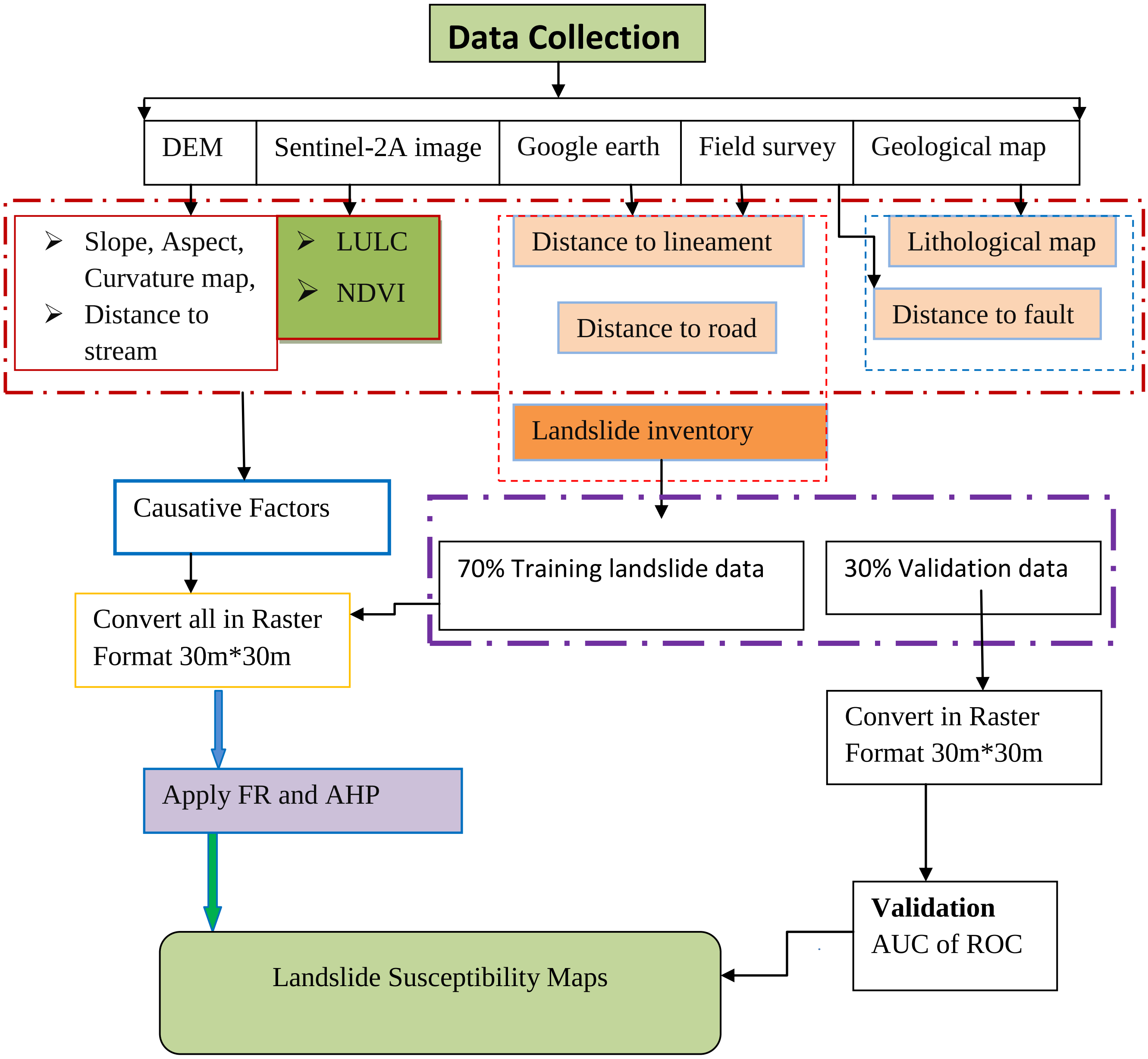

Figure 3.4 General flow chart of the study

4. RESULT AND DISCUSSION

4.1 Landslide Inventory

A comprehensive landslide inventory was created by interpreting Google Earth imagery, identifying and mapping 793 landslides within the study area. Using ArcGIS software, the vector-based landslide inventory was converted into a raster format with a pixel size of 30 meters by 30 meters. The resulting raster dataset was randomly split into two subsets: 70% (555 landslides) for susceptibility prediction modeling and 30% (238 landslides) for model validation. The spatial distribution of landslides within the study area is concentrated in the northern, northeastern, middle part and southeastern regions, characterized by rugged topography, steep slopes, deep gorges, and fractured and weathered bedrock. The identified landslides encompass various types, including debris slides, rotational and translational slides, rock slides, creep, and earth slides.

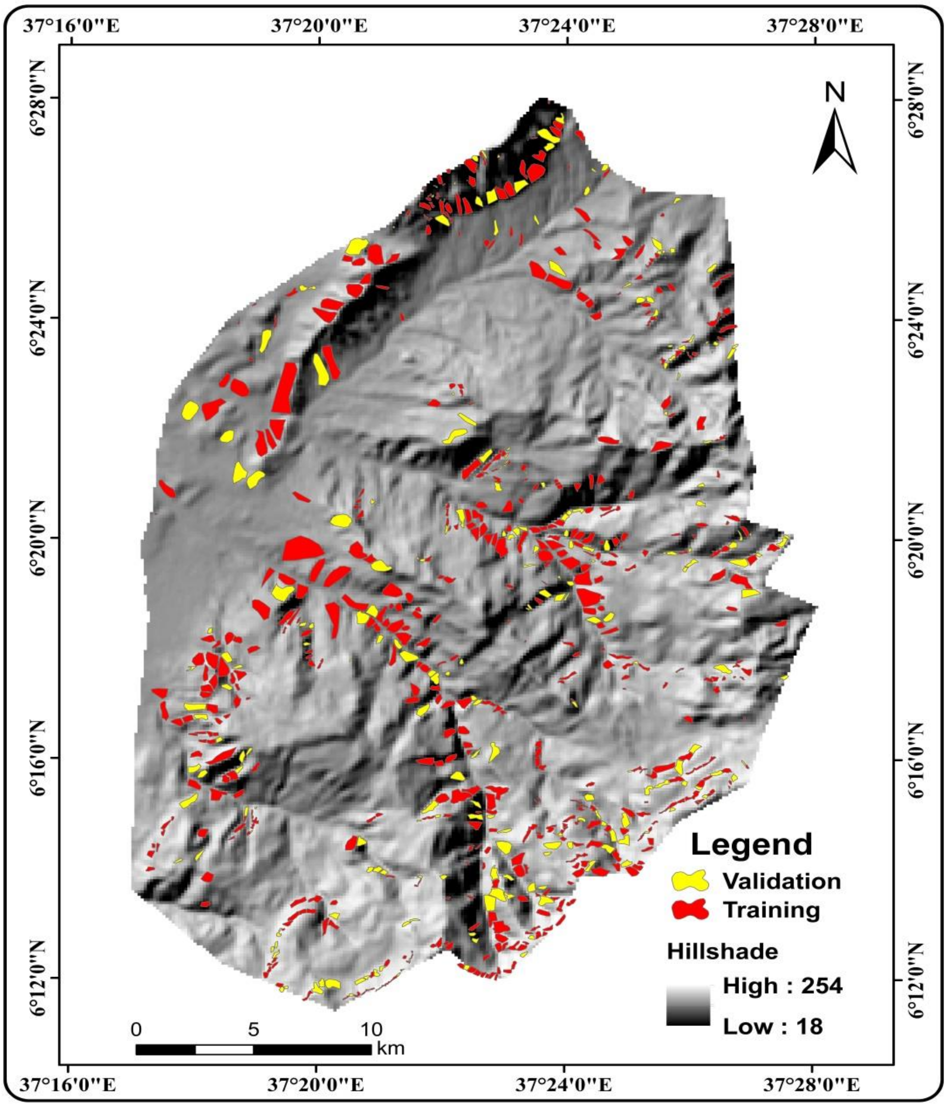

Figure 4.1 Landslide inventory map of the study

4.2 Landslide types and failure mechanism in different localities of study area

During field surveying, several active landslides were identified. Most of them are distributed along roads, near rivers, and around the steep slopes in the study area. Among these several landslides, currently there are four extremely damaged sites that damage infrastructure and are also the causes of agricultural damage. These four extremely damaged sites; landslides in Wulokode locality, landslides in Dida locality, landslides in Gebako locality, and landslides in Menena locality in the study area were selected for a detailed discussion because of its high magnitude of damage. Even though all inventoried landslides have their own effects on the local people and infrastructure, it is impossible to discuss them all. Among those several landslides, four extremely damaged sites are discussed separately.

Landslide in Wulokode locality

This area is mainly characterized by a moderate to gentle slope, and it is exposed to many road cuts and hill sides as indicated in plate 1 (a and b). The lithology of the area is covered by highly weathered basalt, and basalt is overlaid by residual soil and stick clay soils. During the field work, many roads were cut and much ground water was observed at the surface in this village, which indicated that the groundwater in this area is shallow. The common type of landslide that was observed in this village during field work is a progressive basalt and soil slide with an average landslide depth of 5–10 m and a width of 5–15 m. The slide of this area is active and old, which occurred due to human activity, overuse of cultivation, improper slope cut for road construction, ground water observed at the surface, and stream cut below the road of sheet erosion. According to villagers, landslide occurrences in this area are very high during rainy seasons, causing damage to cultivated land that was covered by crop vegetation. The common types of landslides that were observed in these villages are debris slides and rockslides.

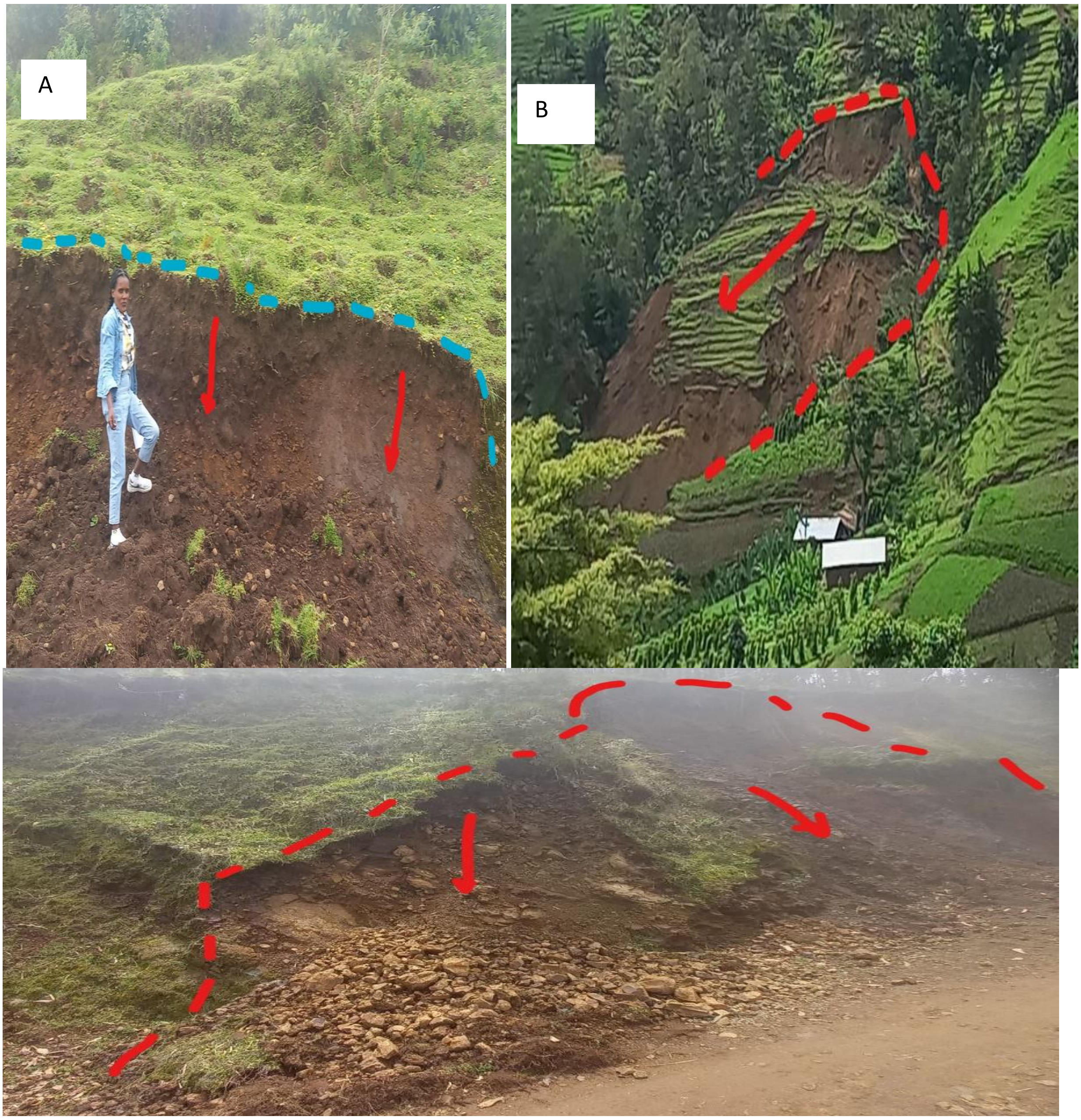

Plate 1 A and B) debris slide and C) rock slide in the locality

Landslide in Dida locality

This area is mainly characterized by moderately steep and very steep-sloped topography. The slope in the village is composed of ryholite rock, overlaid by residual deposits and basalt. The topography, road cuts, stream undercutting, erosion, and farming practices in this village have severely impacted its landscape. Based on information gathered from the villager, the most common types of landslides that were observed in this village during field work were debris falls and rock falls of active and old landslides.

The landslides that occurred in these villages are due to the steepness of the slope, road cuts, heavy and prolonged rainfall, and stream undercutting, which caused damage to vegetation, and various crops in the village as indicated in plate 2 (A and B).

Plate 2 A) Rock fall and B) debris fall

Landslide in Gebako locality

This area is mainly characterized by a moderately gentle to steep slope, and it is exposed to many road cuts, river cuts and hill side topography. The lithology of the area is covered by quaternary deposits and pyroclastic rock overlain by quaternary deposits. During the field work, many roads were cut and much of river cuts there in this village. The common type of landslide that was observed in this village during field work is a progressive pyroclastic fall and rock fall of plate 3 (A and B) respectively, with an average landslide depth of 10–40 m and a width of 20–100 m. The slide of this area is active and old, which occurred due to human activity, overuse of cultivation, improper slope cut for road construction, ground water observed at the surface, and stream cut of Woyiza Dacea River near the stream topography cause erosion at the toe. According to villagers, landslide occurrences in this area are very high during rainy seasons, causing damage to cultivated land that was covered by crop vegetation.

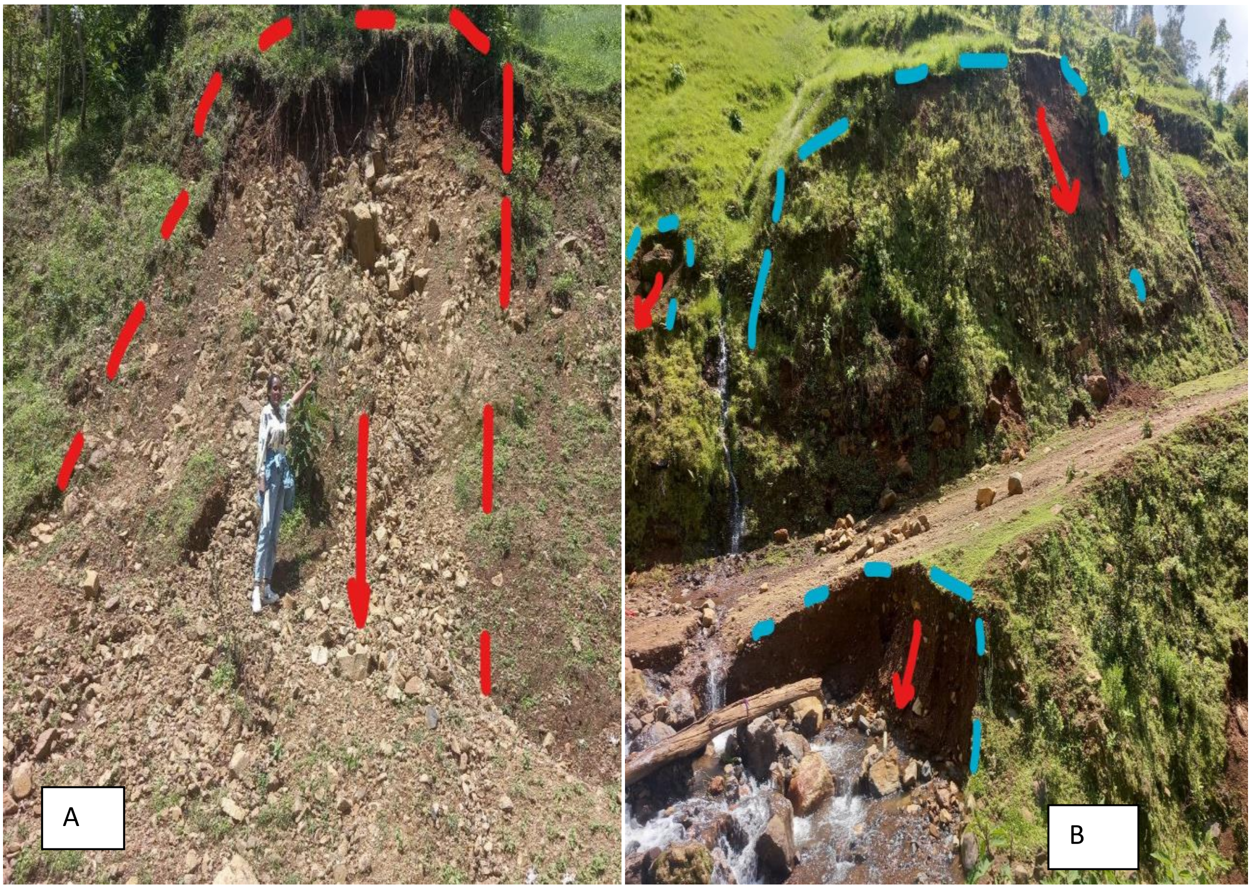

Plate 3 A) pyroclastic fall and B) rock fall under stream cut

Landslide in Menena locality

This area is mainly characterized by a gentle to steep slope, and it is exposed to many road cuts, river cuts, and hill sides. The lithology of the area is covered by highly weathered rhyolite, quaternary deposits, and rhyolite. During the field work, roads and rivers were cut, and much ground water was observed at the surface in this village, which indicated that the groundwater in this area is shallow. The common type of landslide that was observed in this village during field work is a progressively moving rhyolite with an average landslide depth of 5–20 m, a width of 15-200 m, and 20–100 m. The slide in this area is active and old, which occurred due to improper slope cuts for road construction, ground water, gravity, and stream cuts near hill sides. There was erosion near the Tsio and Gazote rivers. The common types of landslides that were observed in these villages are debris slides and creep as shown in plate 4 (A, B and C). To stabilize the slides in this area, retaining walls were provided, but they are not effective; in fact, the retain walls are damaged because they were provided without proper investigation study on the effects of applying these preventive measures on aggravating further landslide occurrences as shown Plate 4(c).

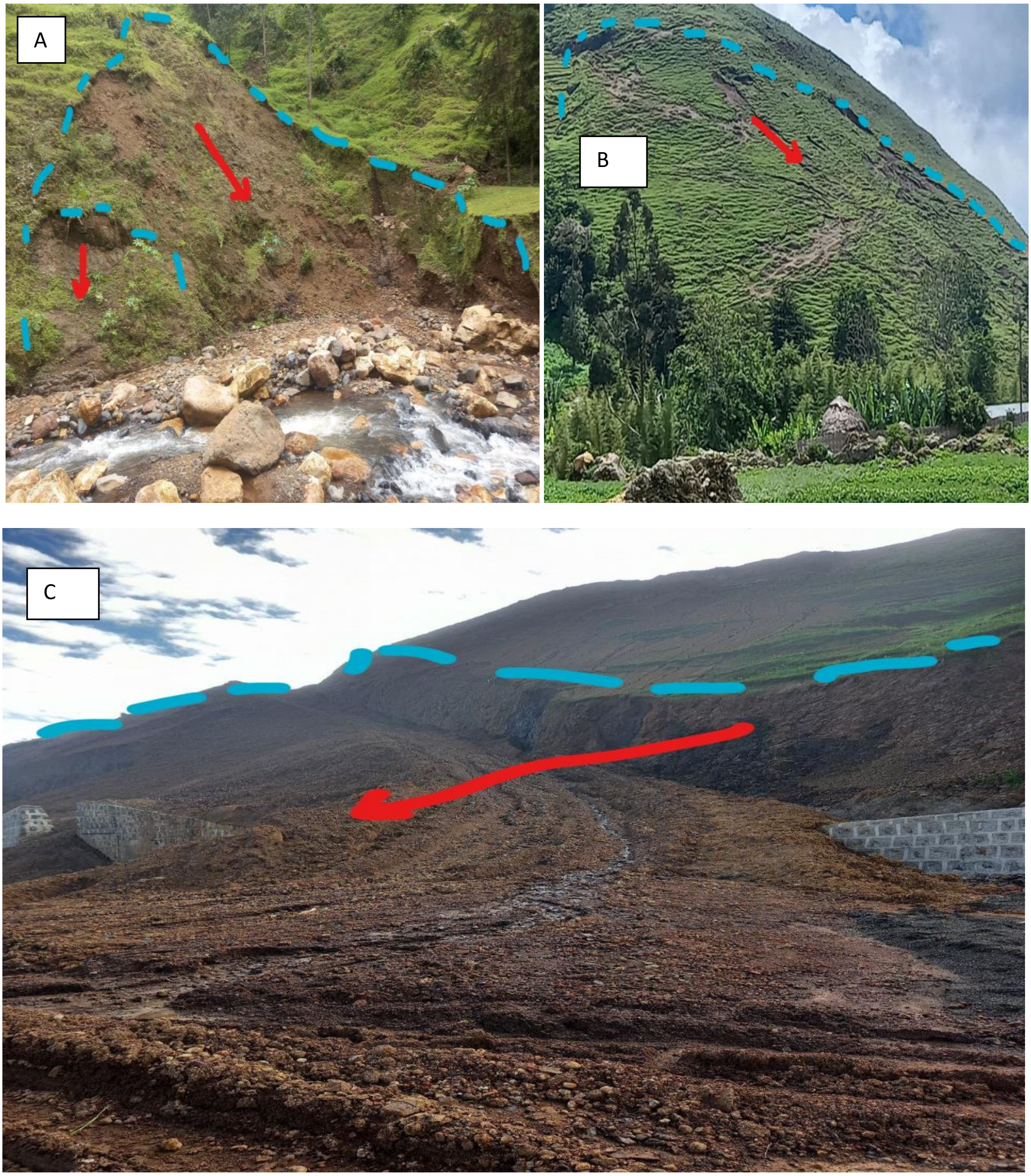

Plate4 A) Debris slide of stream under cutting, B) creep and C, debris slide of road cutting

4.3 Landslide causative factor analyses

Landslides are spatially distributed and have a high density depending on the topography, weather, geology, land use and anthropogenic causes (Khan et al., 2019). In order to understand how the landslides occur and subsequently create a map of landslide susceptibility, it is crucial to evaluate the impact of these causal factors based on the spatial distribution of landslides. In the present study, slope, aspect, curvature, distance to lineament, distance to stream, distance to road, distance to fault, land use/land cover, normalized difference vegetation index (NDVI), lithology and rainfall have been considered as causative elements and all except rainfall were used to prepare landslide susceptibility mapping. The following will provide a detailed explanation of how each causative factor influences the landslide occurrence.

4.3.1 Slope

Steepness of the land is a major influence in setting the stage for landslides (Kumar et al., 2015). When assessing landslide risk, slope is crucial. It not only influences where houses and roads should be built, but also how the land is prepared to withstand potential slides. As slope angles increase, the probability of landslide occurrence increases as the slope angle decreases due to gravity, resulting in a lower frequency of landslide events on gentler slopes compared to steeper ones (Kumar et al., 2015). Steeper slopes are typically characterized by a greater susceptibility to sliding (Hamza and Raghuvanshi, 2016). In this study, slopes were classified into five categories (0° - 7°), (7° - 17°), (17° - 28°), (28°- 40°) and > 40°based on the natural breaks' method, as it clearly classifies the slope with the existing topography of the study area in comparison with other classification methods (Meten et al., 2015) Figure 4.2(A).

The study found that as the slope angle increases, so does the frequency of landslides, and has a lower percentage of landslides compared to steeper slopes except for the first class. This confirms that slope steepness is a major factor in landslide occurrence (Asmelash and Barbieri, 2012; Ayele, 2014). Several studies support this observation, highlighting the importance of slope angle in landslide susceptibility assessments (Raghuvanshi et al., 2015; Erden and Karaman, 2012).

4.3.2 Aspect

Aspect is the direction in which the maximum slope of the terrain is oriented (Xu et al., 2012) and considered as key factor for landslide occurrence (Yalcin, 2011). It is often quantified in terms of degrees from 0 to 360^0, signifying slope orientation (Mersha and Meten 2020). The slope aspect might affect the beginning of a landslide as it affects moisture retention and vegetation cover (Raghuvanshi et al. 2015). The aspect of the study area is classified into N, NE, NW, S, SE, SW, E, W and flat. The aspect factor map was derived from the DEM of the study area with a spatial resolution of 30m * 30m. The aspect map was grouped into nine classes Flat (-1°), North (0°-22.5°; 337.5°-360°), Northeast (22.5°-67.5°), East (67.5°-112.5°), Southeast (112.5°-157.5°), South (157.5°-202.5°), Southwest (202.5°-247.5°), West (247.5°-292.5°) and Northwest (292.5°-337.5°) as shown in Figure 4.2(B)

The results revealed that 29.12% of the landslide occurred in the north-facing slopes, 11.29% occurred in the south-facing slopes while 10.10% in the east-facing and 7.94% in the northwest facing slopes. This shows that slopes facing the north, south, east, and northwest have a high correlation with landslides. This result agrees with a study conducted by Chimidi et al. (2017) in which slopes oriented towards southwest, west, and northwest showed a high probability of landslide occurrence. The result was in line with Shano et al. (2021), who reported the north, northeast, south, and southwest aspect classes as the most landslide-prone classes.

4.3.3 Curvature

The curvature of the study area was derived from a digital elevation model (DEM) with a spatial resolution of 30 meters, and it was categorized into three classes: Large negative values represent concave curvature; values near zero indicate flat terrain; and large positive values signify convex curvature. Among the total area, flat curvature is the most dominant one, which covers a large area as compared to the concave and convex ones, respectively Figure 4.2(C). As a result, concave and convex aspect classes are highly influencing the landslide occurrence as compared to the flat curvature. Accordingly, the maximum values were assigned for the curvature classes within negative and positive values. These curvature classes are zones of groundwater accumulation and divergence, respectively. The negative values are zones of groundwater percolation into the soil/rock mass. Further, a flat area was assigned with the lowest susceptibility to landslide, which agrees with Girma (2015), Chen et al. (2016), and Ayele (2019) in which landslide activity increases with negative and positive values of curvature.

4.3.4 Lithology

Lithology serves as one of the contributing factors to landslides (Riaz et al., 2018; Berhane et al., 2020). Landslide susceptibility tends to rise when the underlying rock unit is loose and fractured.

The results of lithology from the existing map and field survey showed that the study area contains three lithological units, namely Quaternary Alluvial Deposit (QAD), Basalt, and Rhyolite Figure 4.2(D). The result showed that basalt covered the highest area coverage and landslide coverage in percent. But rhyolite had less area coverage and landslide percentage, as shown in Table 3.

Table 3 Area coverage of each lithological unit

Lithology	Area (km^2)	Area (%)
Basalt	388.80	88.17
Quaternary Alluvial Deposit	14.66	3.32
Rhyolite	37.50	8.50

Basalt

The basalt lithological units of the study area ranged from a gentle to a steep slope topographically. As indicated in Table 3 above, the basalt lithological unit of the study covered a large area of 388.80 km^2 and 88.17 percent of the total area. This lithological unit had a large thickness, which was overlaid by the quaternary alluvial deposit at the western part, the ryholite unit at the southeast, and some at the northern part of the study area.

Quaternary Alluvial Deposit

This lithological unit covered a small area of the total area of the study area by 14.66 km^2 and 3.32 percent, as shown in Table (3). This unit was founded in the western parts of the study area and had a small thickness, which was underlie by the basalt lithological unit.

Ryholite

Ryholite in the study area forms a very steep slope and cliff. This unit covered 37.50 km^2 and 8.50 percent of the total area, and it was exposed in the southeastern and northern parts of the study area. The unit had a moderate thickness, which was underlie by the basalt lithological unit.

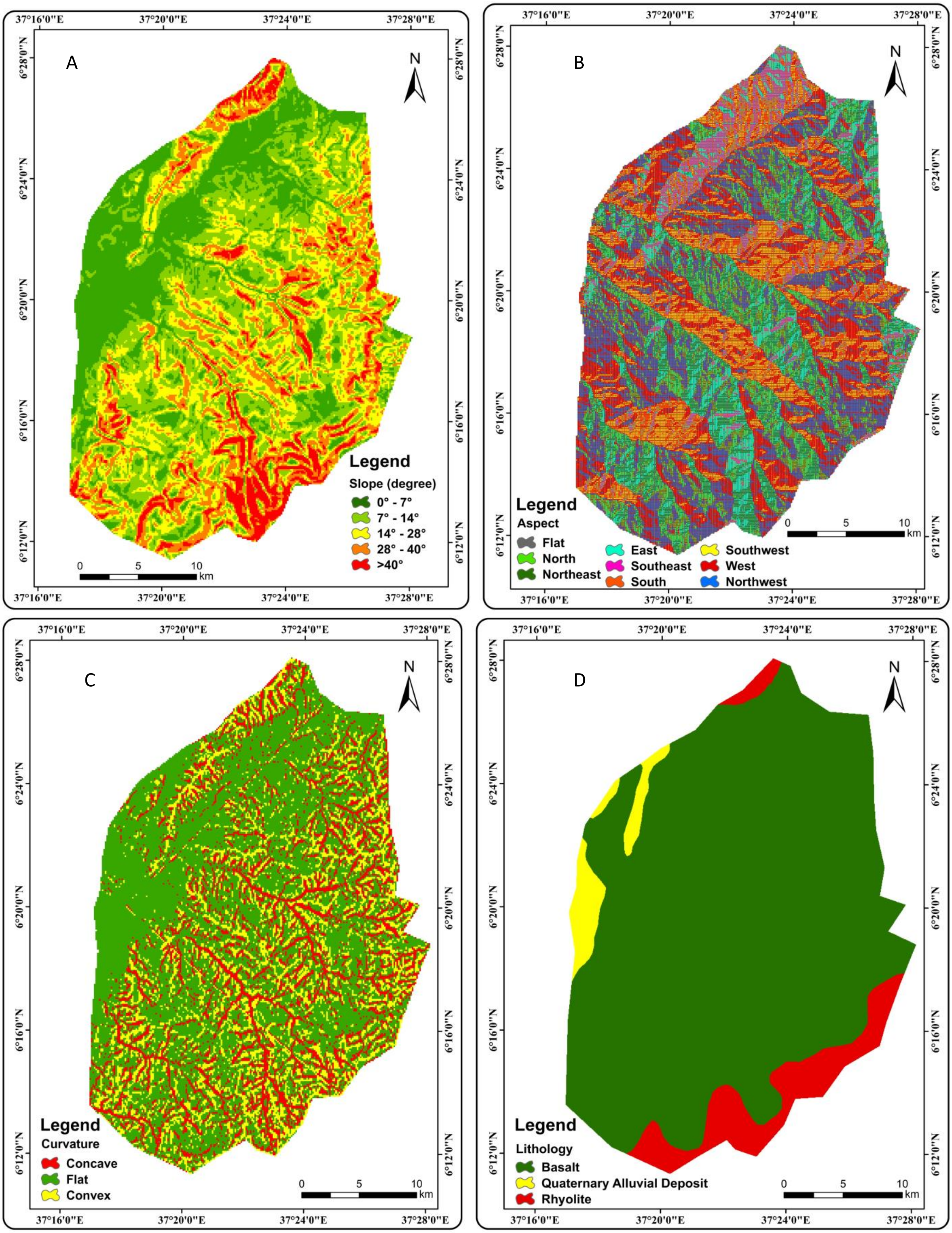

Figure 4.2 A) Slope, B) aspect, C) curvature and D) Lithology maps

4.3.5 Land use/land cover

Land use/land cover changes significantly influence globally on rainfall-triggered landslides (Mersha and Meten, 2020). The result showed that Land use/land cover of the study area classified in to five classes: sparse forest, shrub, bare land, agricultural land, and settlement with an agricultural land predominating in the area Figure 4.3(A). The result indicated sparse forest, agricultural land, bare land, and shrubs had percentage values of 17.480 %, 45.704 %, 11.989 %, and 24.828 %, respectively, which revealed the highest probability of landslide occurrence, which was in line with Sharma et al. (2012), who reported that sparsely vegetated or barren slopes are prone to erosion, thereby intensifying slope instability and in line with the founding of Addis (2022), who reported that bare land and sparse forest areas were highly susceptible to landslides. But settlement had a lower probability of landslide occurrence with a value of zero percent (0%).

4.3.6 Normalized Difference Vegetarian Index

The NDVI of the study was classified into five classes: -0.128 – 0.144, 0.144 – 0.200, 0.200 – 0.269, 0.269 – 0.358 and 0.358 – 0.636, as shown in Figure 4.3(B). The result indicated that the -0.128–0.44, 0.144–0.200, and 0.200–0.269 classes had a lower value of NDVI and had the highest percentage of landslide occurrence and the highest probability of a landslide. These results were similar to those of Addis (2022), who reported that lower values of NDVI had the highest probability of a landslide and higher values of NDVI had the lowest probability of a landslide. This class of NDVI means bare land, built-up areas, and shrubs that were exposed to erosion and soil moisture. However, the remaining NDVI classes had higher NDVI values, with relatively high vegetation coverage and a lower probability of landslide occurrence, because vegetation increases soil strength through its root system and reduces the risk of shallow landslides.

4.3.7 Distance to stream

Streams play a crucial role in landslide susceptibility, especially when they undercut slope bases (Che et al., 2011). For this study area, the distance to stream was generated from a DEM of 30 m by 30 m resolution and classified into seven classes: 0 – 100m, 100m – 200m, 200m – 300m, 300m – 400m, 400m -500m, 500m - 600m, > 600m based on manual classification methods, because manual classification is realistic, the relationship between stream and landslide occurrences. The result indicated that as distance to the stream decreased, the probability of land slide occurrence increased because the stream can erode the slopes or saturate the lower part of the material, resulting in increased water levels, which may adversely affect stability. All classes of distance to stream have the highest probability of land slide, except the last class > 600m as shown in Figure 4.3(C). The result was similar to the finding of Addis (2023), who found the probability of landslide occurrence increases as the distance to the stream decreases.

4.3.8 Distance to lineament

Lineament geometry and fault rupture have a direct influence on the distribution of landslides (Mahmood et al. 2015; Riaz et al. 2018). The lineament factor was characterized as proximity analysis by the use of the Euclidian distance buffering tool, and the distance to lineament factor was reclassified based on manual classification methods into seven classes: 0-50m, 50-100m, 100-150m, 150-200m, 200m-250m, 250m-300m, and >300m. The classification was made with manual classification to be realistic about the relationship of landslides with escarpment. The results showed that the lineament class of 0–50 m had a higher probability of landslide occurrence, whereas the lineament class of > 300m had a lower probability of landslide occurrence, as shown in figure 4.3(D).The result was similar to the finding of Genene and Meten (2021), who found the probability of landslide occurrence increases as the distance to the lineament decreases.

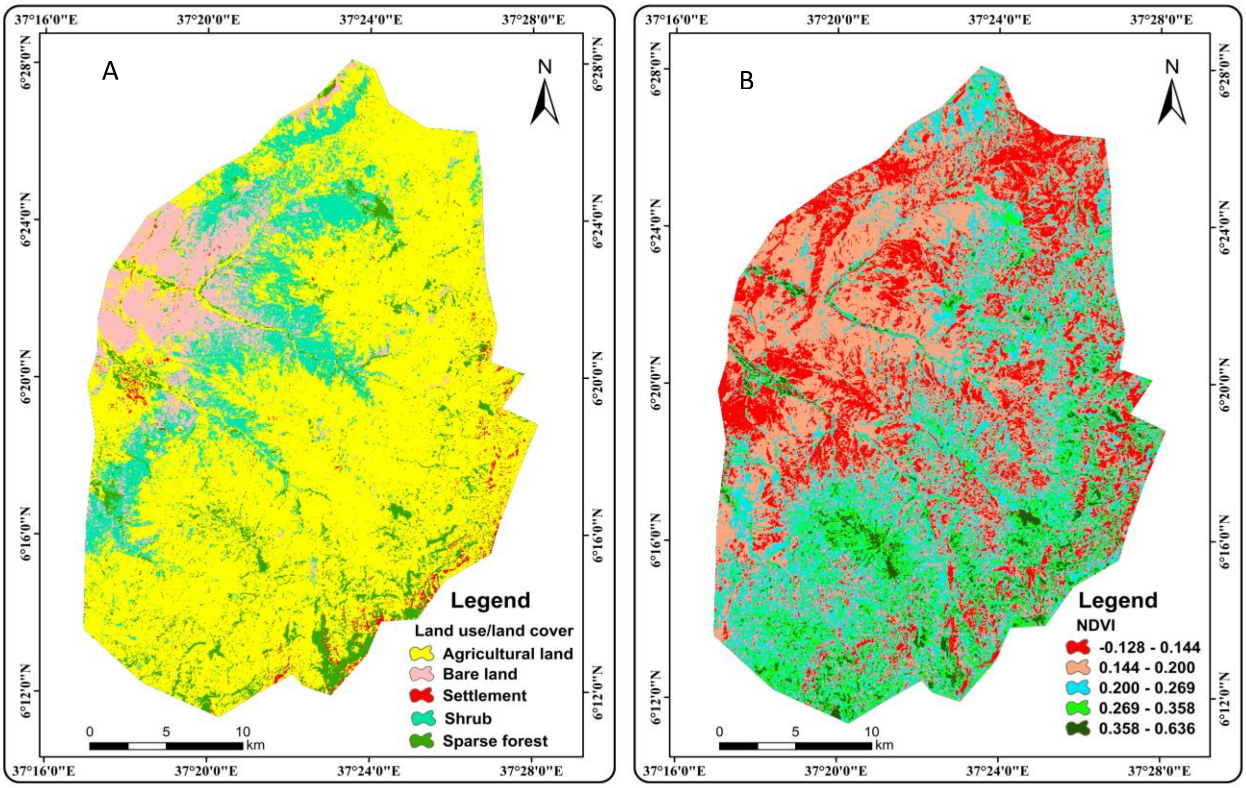

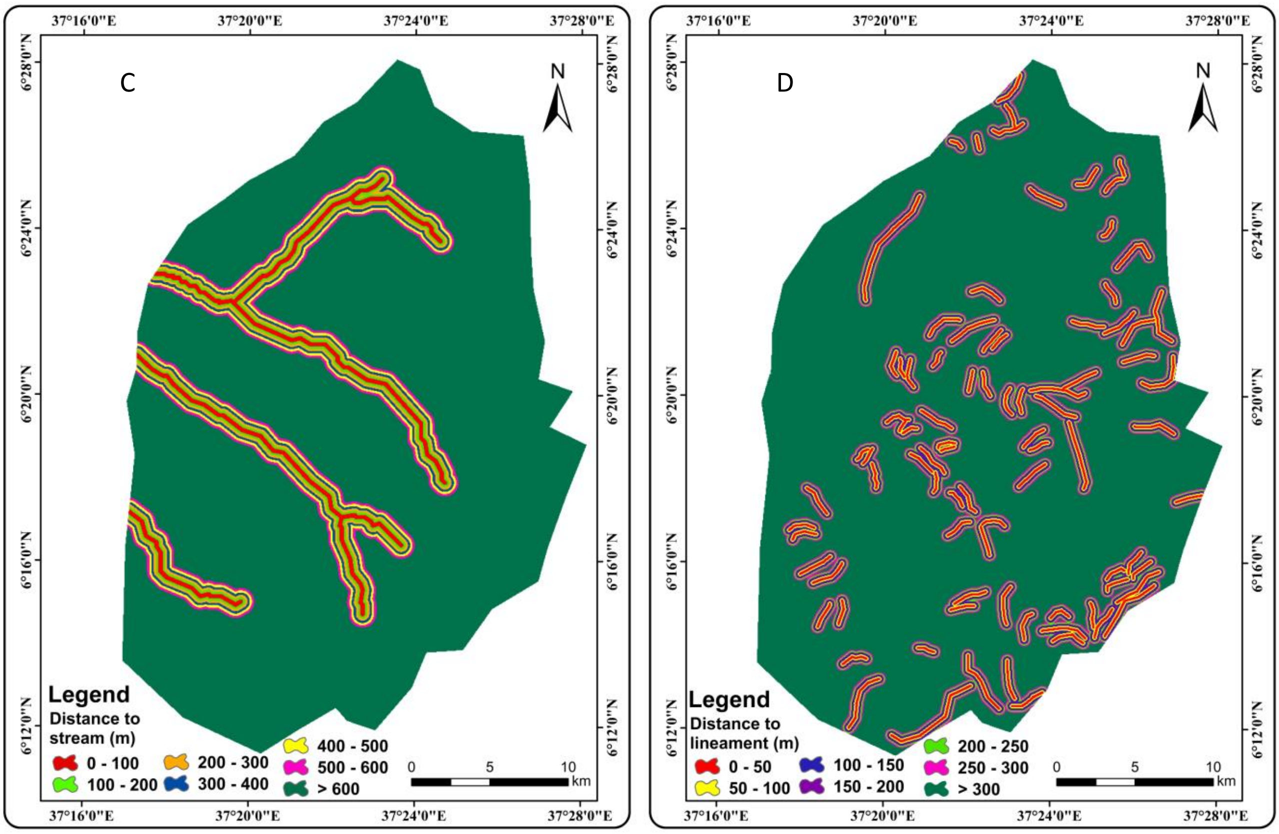

Figure 4.3 A) LULC, B) NDVI, C) distance to stream and D) Distance to lineament Map

4.3.9 Distance to road

Distance to road was a critical and important element that was considered because of the terrain and the infrastructure properties that were undertaken to mitigate landslide risk in the study area. Road cuts at the outset decrease the general stability of the slopes and increase depending on the dip directions (Michael and Samanta, 2016). Distance to road of the study was classified into seven classes: 0–100 m, 100–200 m, 200–300 m, 300–400 m, 400–500 m, 500–600 m, and > 600 m by manual classification. The result revealed that the distance to road of class 0–100m had a higher probability of landslide occurrence, but class > 600m had a lower probability of landslide occurrence, as shown in figure 4.4(A).

4.3.10 Distance to Fault

The presence of strongly weathered rocks and a well-developed fault structure within the study area creates favorable conditions for landslides (Li et al., 2015). To quantify this influence, the distance to faults was classified into seven categories at 100-meter intervals: 0–100 m, 100–200 m, 200–300 m, 300–400 m, 400–500 m, 500–600 m, and > 600 m Figure 4.4(B). As expected, closer proximity to faults generally increases the probability of landslide occurrence, which is similar to Pradhan et al. (2012), who found the risk of a landslide increases as the distance from the fault decreases. The result revealed that the structure of rock and soil in the fault zone is fractured and easily weathered, affecting landslide disasters.

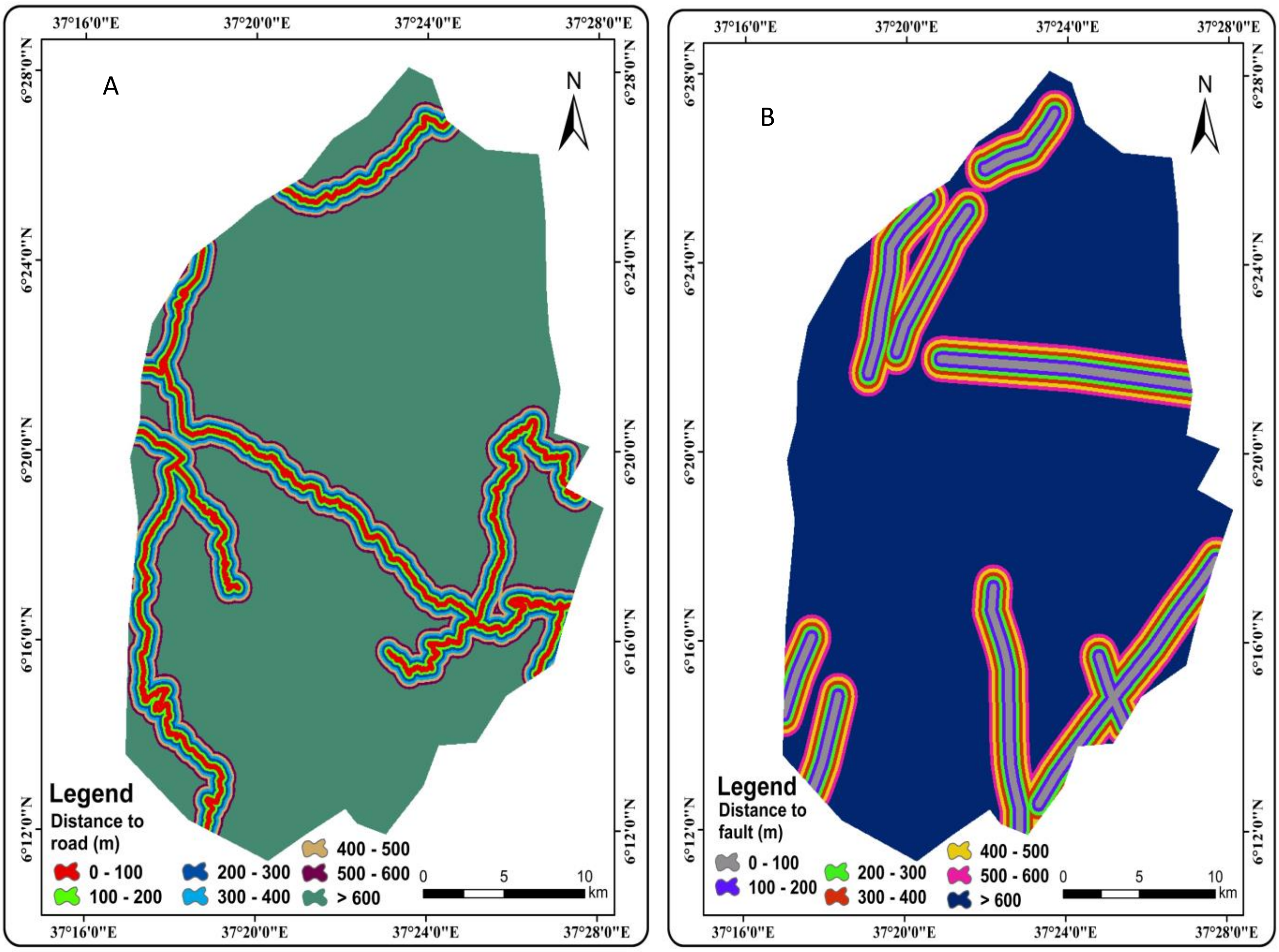

Figure 4.4 A) distance to road and B) Distance to fault Map

4.4 Results of Frequency ratio analysis

4.4.1 Relationship between landslide and causative factors

Using the statistical frequency ratio and analytical hierarchy process, this study examined the relationships between ten potential causes of landslides. The causal factors were classified into fifty-eight classes (Table 4), which assigns the weights assigned to each class of the FR model. The weight values obtained from the FR model illustrate the spatial relationship of the causative factor classes to landslide occurrence. In this study, the relationship between landslides and each class of causative factors (slope, aspect, curvature, and distance to stream, distance to lineaments, distance to road, and distance to fault, lithology, land use/land cover and NDVI) was examined and shown in the following figure (Figure 4.5).

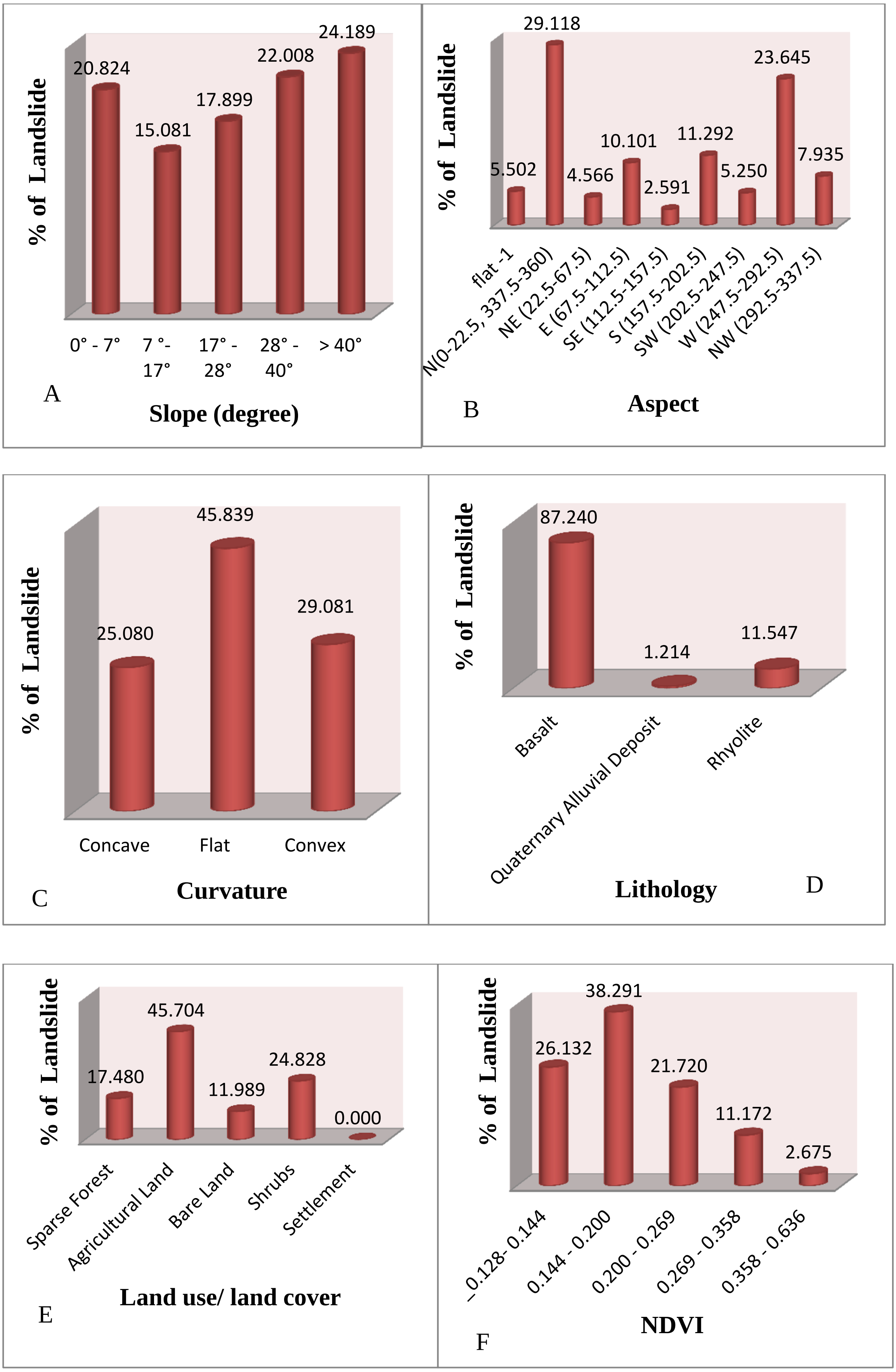

% of Landslide
20.824
15.081
17.899
22.008
24.189
0° - 7°
7 °- 17°
17° - 28°
28° - 40°
> 40°
A
Slope (degree)
% of Landslide
5.502
29.118
4.566
10.101
2.591
11.292
5.250
23.645
7.935
flat -1
N(0-22.5, 337.5-360)
NE (22.5-67.5)
E (67.5-112.5)
SE (112.5-157.5)
S (157.5-202.5)
SW (202.5-247.5)
W (247.5-292.5)
NW (292.5-337.5)
B
Aspect
% of Landslide
25.080
45.839
29.081
Concave
Flat
Convex
C
Curvature
% of Landslide
87.240
1.214
11.547
Basalt
Quaternary Alluvial Deposit
Rhyolite
Lithology
D
% of Landslide
17.480
45.704
11.989
24.828
0.000
Sparse Forest
Agricultural Land
Bare Land
Shrubs
Settlement
Land use/ land cover
E
% of Landslide
26.132
38.291
21.720
11.172
2.675
_0.128- 0.144
0.144 - 0.200
0.200 - 0.269
0.269 - 0.358
0.358 - 0.636
NDVI
F

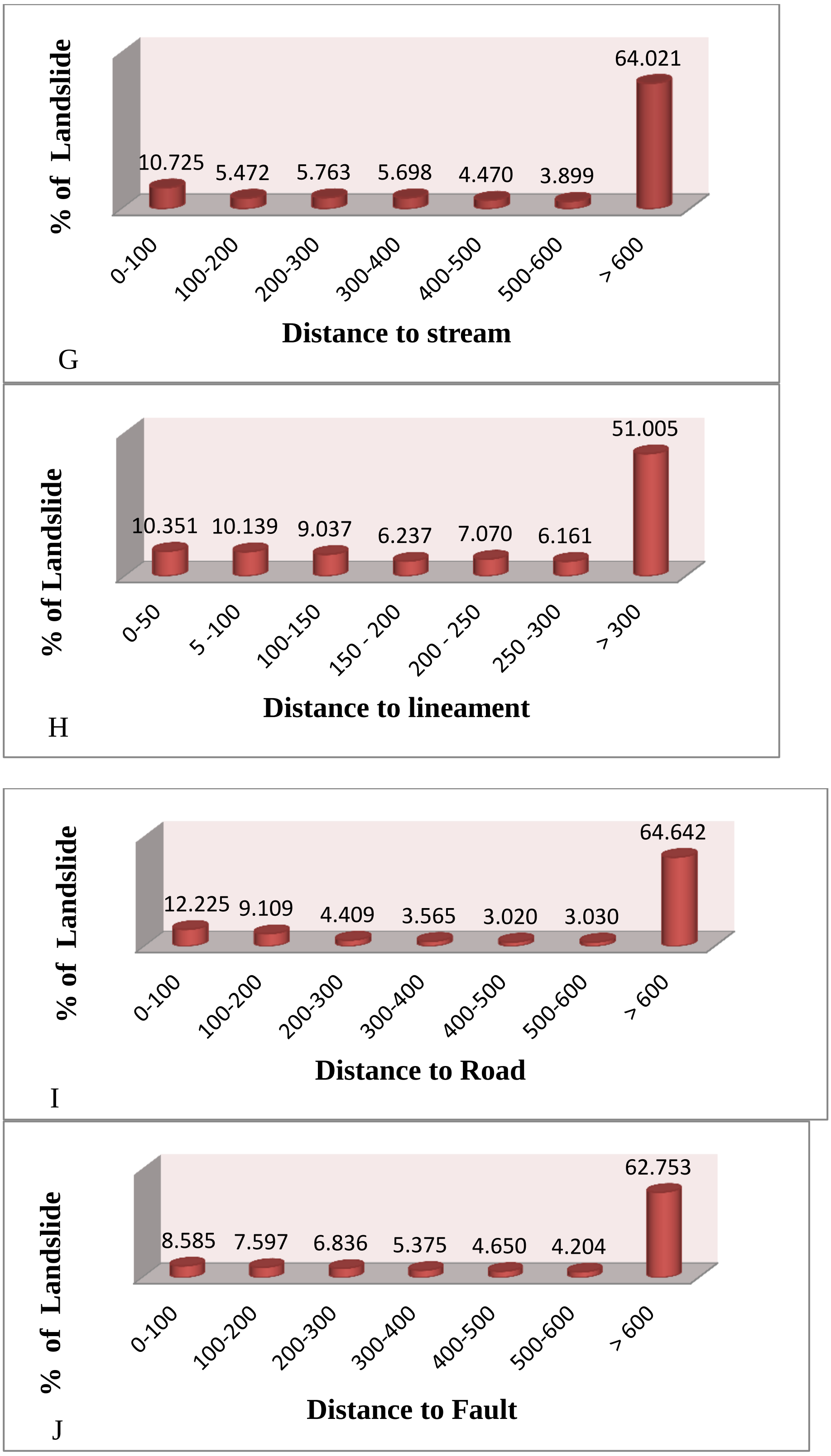

Figure 4.5 A), slope, B), aspect, C) curvature, D) lithology, E) LULC, F) NDVI, G) distance to stream, H) distance to lineament, I) distance to road and J) distance to fault relationship with the percentage of landslide occurrence of the frequency ratio approach

4.4.2 Rating Landslide Factors using Frequency Ratio Approach

The FR values increase with increasing slope angle. For example, the slope classes of 28° - 40°, >40° have the highest FR values of 1.40 and 2.75, respectively. However, the classes 0° - 7°, 7°-17°, 17°-28°, with lower slope angles have the least FR values with the least probability of landslide occurrence. The results agree with the finding of Mersha and Meten (2020) found that slope classes > 12^0 have a higher contribution to landslide occurrence (This correlation indicated that the landslide probability increases as the slope gradient increases and similar with Genene and Meten (2021) who reported slope classes >15^0 had high probability of landslide. The aspect analyses showed that the maximum FR value (4.26) was for the North, followed by South (1.12), West (1.03), Southwest (1.01), and Northeast (1.0), indicating a higher probability of landslide occurrence. The other aspect classes have less than zero FR values, which indicate a lower probability of landslide occurrence. The results in this study area in agreement with Getachew and Meten (2021), in which the north, southwest, west, and northwest face a high probability of landslide occurrence. This is also in line with Addis (2022), which reported that the southwest, west, and northwest-facing slopes had a high probability of landslide occurrence.

In the case of curvature, the FR is higher for a concave (1.57), and for a convex slope, the FR value is 1.43. The other curvature (flat) indicates lower values (0.72). This agrees with Mersha and Meten (2020) reported that concave and convex slopes have high probability of landslide occurrence due to the effects of slope shape for rainwater impounding and gravity effect.

The FR for distance to stream clearly showed that the class of 0 - 100m, 100 - 200m, 200 – 300m, 300 – 400m, and 400 – 500m, and 500m – 600m have the highest influence on landslide occurrence with values of 4.02, 2.03, 2.16, 2.16, 1.68, and 1.46 respectively. The remaining classes of above 600m have a lower probability of landslide occurrence with FR values of 0.76.

For distance to lineaments, the intervals 0 – 50m, 50 – 100m and 150 – 200m, 200m – 250m, and 250m – 300m have a higher probability of landslide occurrence with values of 3.24, 2.84, 2.38, 2.08, 1.87, and 1.68, respectively. The FR for distance to road, the interval 0 – 100m, 100m – 200m, 200m -300m, and 300m - 400m have a higher probability of landslide occurrence with FR value of 2.58, 2.28, 1.05, and 1.0 respectively. FR value for distance to fault indicated, the interval of 0 – 100m, 100m – 200m, 200m – 300m, 300m –

400m, 400m – 500m, and 500m – 600m have a higher probability of landslide occurrence with values of 1.87, 1.75, 1.54, 1.23, 1.09, and 1.01, respectively. For the lithology factor, frequency analysis shows that the basalt and rhyolite have the highest susceptibility to landslides with FR values of 1.0 and 1.36, respectively. For land use and land cover, shrub and sparse forest have higher FR values of 2.160 and 4.410 respectively. For normalized difference vegetation index, classes of -0.128 – 0.144, 0.144 – 0.200, and 0.200 – 0.269 have higher probability of landslide occurrence with FR value of 1.03, 1.05, and 1.02 respectively.

Table 4 Rating of each factor class from a spatial relationship between each factor class and landslide using frequency ratio model

Factor	Class	C P	% CP	LP	% LP	SR(a)	CR(b)	FR=a/b
Slope	0° - 7°	138858	28.532	5787	20.824	0.208	0.285	0.73
	7°-17°	124716	25.626	4191	15.081	0.151	0.256	0.59
	17°-28°	103951	21.359	4974	17.899	0.179	0.214	0.84
	28° - 40°	76301	15.678	6116	22.008	0.220	0.157	1.40
	>40°	42854	8.805	6722	24.189	0.242	0.088	2.75
Aspect	flat -1	133181	27.365	1529	5.502	0.055	0.274	0.20
	N(0-22.5, 337.5-360)	33295	6.841	8092	29.118	0.291	0.068	4.26
	NE (22.5-67.5)	22198	4.561	1269	4.566	0.046	0.046	1.00
	E (67.5-112.5)	49614	10.194	2807	10.101	0.101	0.102	0.99
	SE(112.5-157.5)	11243	2.310	720	2.591	0.026	0.023	1.12
	S (157.5-202.5)	55331	11.369	3138	11.292	0.113	0.114	0.99
	SW (202.5-247.5)	25219	5.182	1459	5.250	0.053	0.052	1.01
	W (247.5-292.5)	112030	23.019	6571	23.645	0.236	0.230	1.03
	NW (292.5-337.5)	44569	9.158	2205	7.935	0.079	0.092	0.87
Curvature	Concave	78734	16.070	6983	25.080	0.251	0.161	1.56
	Flat	311738	63.627	12763	45.839	0.458	0.636	0.72
	Convex	99475	20.303	8097	29.081	0.291	0.203	1.43
Lithology	Basalt	431695	88.111	24498	87.958	0.880	0.881	1.00
	Quaternary Alluvial Deposit	16586	3.385	738	2.650	0.026	0.034	0.78

	Rhyolite	41666	8.504	3216	11.547	0.115	0.085	1.36
Land use / land cover	Sparse Forest	35908	7.329	4870	17.480	0.175	0.073	2.39
	Agricultural Land	338553	69.098	12733	45.704	0.457	0.691	0.66
	Bare Land	46968	9.586	3340	11.989	0.120	0.096	1.25
	Shrubs	62723	12.802	6917	24.828	0.248	0.128	1.94
	Settlement	5812	1.186	0	0.000	0.000	0.012	0.00
Distance to Lineament	0 - 50	15668	3.198	2883	10.351	0.104	0.032	3.24
	50 - 100	17519	3.576	2824	10.139	0.101	0.036	2.84
	100 - 150	18609	3.798	2517	9.037	0.090	0.038	2.38
	150 - 200	14685	2.997	1737	6.237	0.062	0.030	2.08
	200 - 250	18503	3.777	1969	7.070	0.071	0.038	1.87
	250 -300	18002	3.674	1716	6.161	0.062	0.037	1.68
	> 300	386958	78.980	14206	51.005	0.510	0.790	0.65
Distance to Stream	0-100	13055	2.665	2987	10.725	0.107	0.027	4.02
	100-200	13216	2.697	1524	5.472	0.055	0.027	2.03
	200-300	13056	2.665	1605	5.763	0.058	0.027	2.16
	300-400	12916	2.636	1587	5.698	0.057	0.026	2.16
	400-500	13061	2.666	1245	4.470	0.045	0.027	1.68
	500-600	13086	2.671	1086	3.899	0.039	0.027	1.46
	> 600	411566	84.003	17831	64.021	0.640	0.840	0.76
Distance to Road	0-100	23179	4.731	3405	12.225	0.122	0.047	2.58
	100-200	19577	3.996	2537	9.109	0.091	0.040	2.28
	200-300	20493	4.183	1228	4.409	0.044	0.042	1.05
	300-400	17515	3.575	993	3.565	0.036	0.036	1.00
	400-500	18102	3.695	841	3.020	0.030	0.037	0.82
	500-600	16626	3.393	844	3.030	0.030	0.034	0.89
	> 600	374456	76.428	18004	64.642	0.646	0.764	0.85
Distance to Fault	0-100	22523	4.597	2391	8.585	0.086	0.046	1.87
	100-200	21329	4.353	2116	7.597	0.076	0.044	1.75
	200-300	21772	4.444	1904	6.836	0.068	0.044	1.54
	300-400	21324	4.352	1497	5.375	0.054	0.044	1.23
	400-500	20879	4.261	1295	4.650	0.046	0.043	1.09

	500-600	20466	4.177	1171	4.204	0.042	0.042	1.01
	> 600	361655	73.815	17478	62.753	0.628	0.738	0.85
NDVI	-0.120 – 1.44	124900	25.491	7279	26.132	0.261	0.255	1.03
	0.144 – 0.200	179421	36.618	10666	38.291	0.383	0.366	1.05
	0.200 – 0.269	104559	21.339	6050	21.720	0.217	0.213	1.02
	0.269 – 0.358	58693	11.979	3112	11.172	0.112	0.120	0.93
	0.358 – 0.636	22412	4.574	745	2.675	0.027	0.046	0.58

Where, CP is class pixels, %CP is percentage of class pixels, LP is landslide pixels, %LP, percentage landslide pixels, SR, is slide ratio, CR is Class ratio and FR is frequency ratio

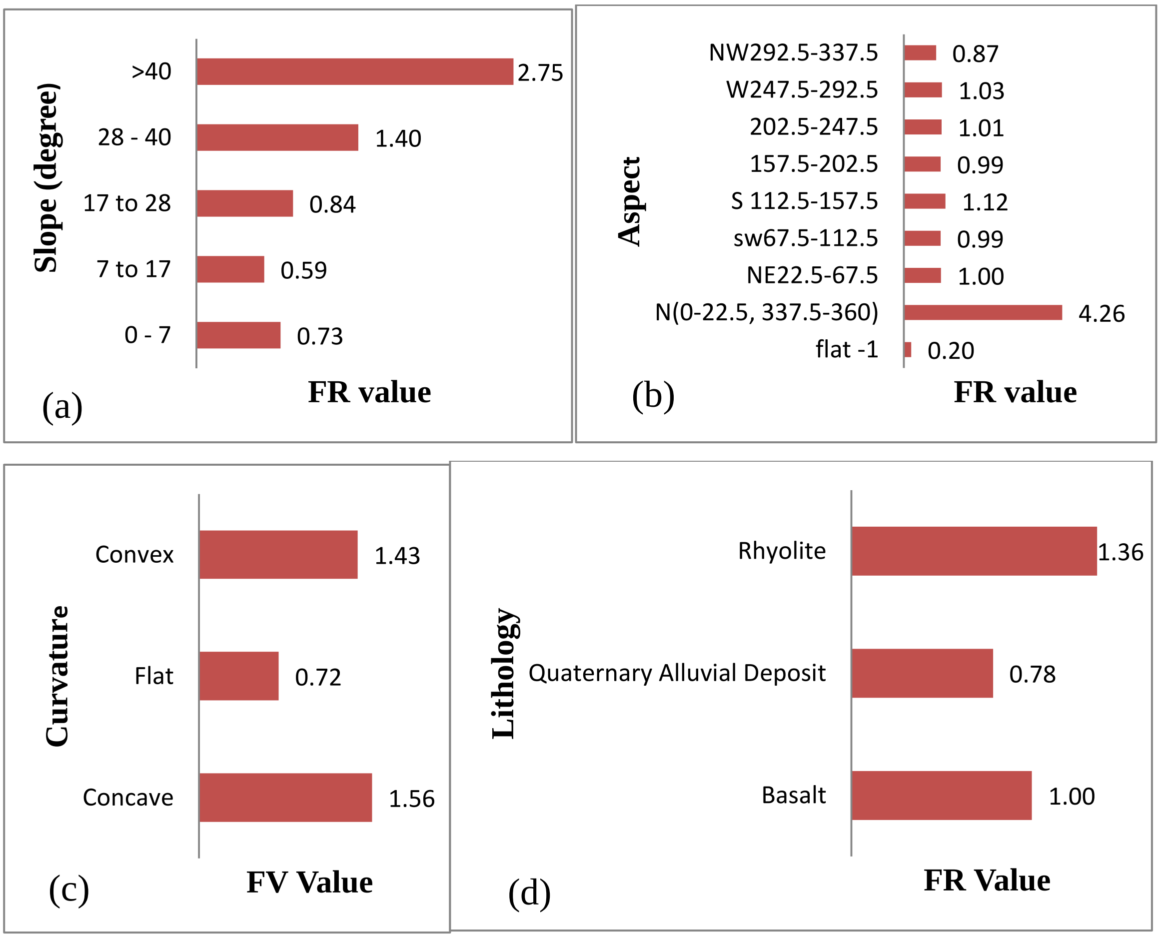

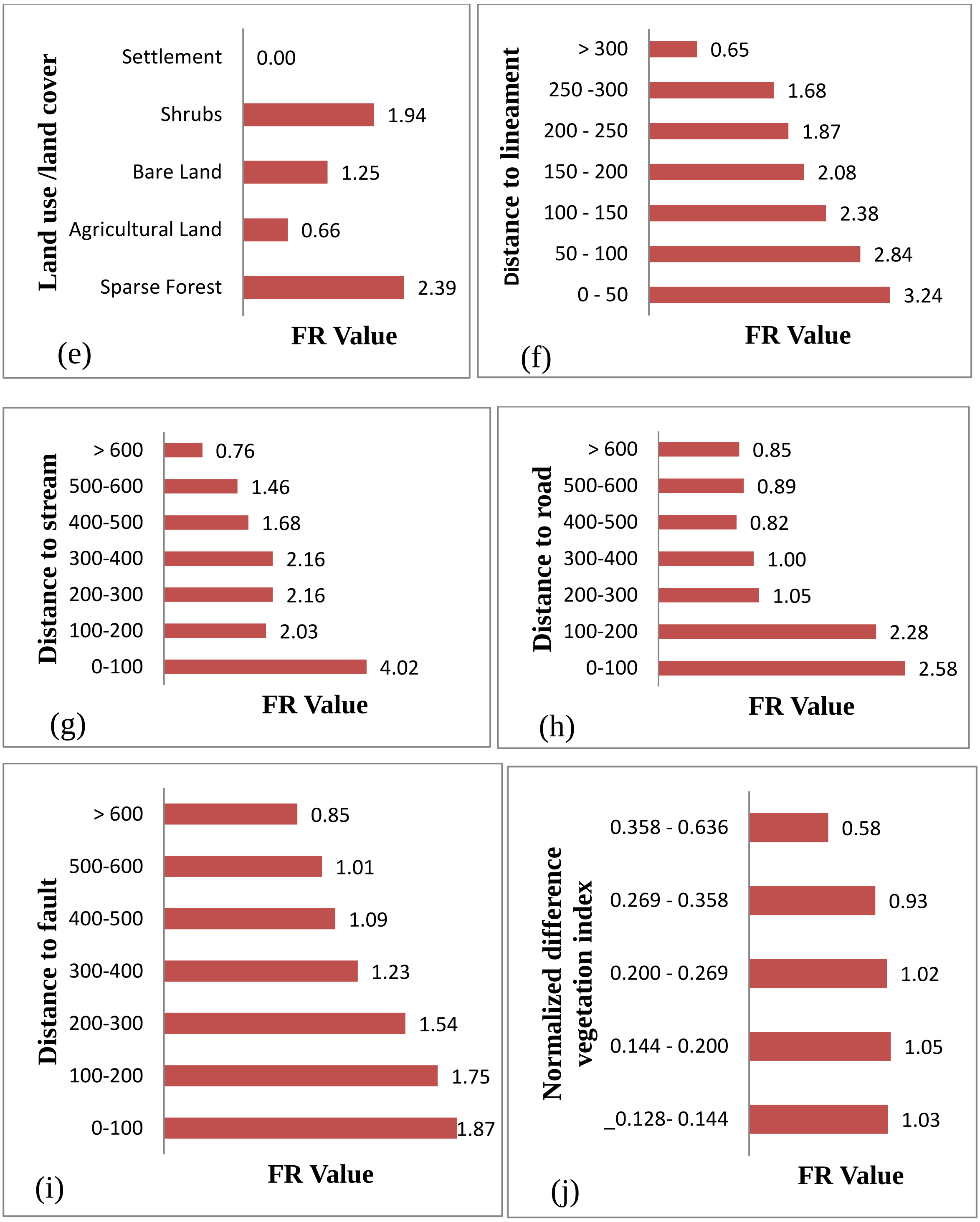

Figure 4.6 Relationship between causative factors and frequency ratio values

4.4.3 Landslide Susceptibility Mapping Using Frequency Ratio Model

From the raster calculation, the final result of LSI values of the study area ranges from 4.52 to 15.43. The LSI map was classified into five classes using the natural breaks method this method is used because it is best for uneven data distribution, and it is capable of classifying the landslide susceptibility index map into a different category based on the inherent data value similarity (Meten et al., 2015). Therefore, the LSI values were classified into five susceptibility areas: very low (4.52 – 6.71), low (6.71 – 7.39), moderate (7.39 – 8.09), high (8.09 – 9.34) and very high (9.34 – 15.43) [Table 5].

Table 5 Frequency Ratio Landslide susceptibility class based on landslide susceptibility index

Susceptibility classes	LSI	Area (km^2)	Area (%)
Very Low	4.52 – 6.71	108.05	24.68
Low	6.71 – 7.39	87.22	19.92
Moderate	7.39 – 8.09	77.09	17.61
High	8.09 – 9.34	81.46	18.61
Very High	9.34 – 15.43	84.01	19.19

The landslide susceptibility map (Figure 4.8 and Table 5) clearly shows that in the study area, 108.05 km^2 (25%) falls in very low susceptible classes and 84.01 km^2 (19%) of the area falls in very high susceptibility classes while the remaining ones including 87.22 km^2 (20%), 77.09 km^2 (18%), and 81.46 km^2 (12%) of the study area fall in low, moderate and high susceptibility classes respectively, were estimated from the ratio of the product of pixels and 30m*30m cell size to 10^6. Where 10^6 is the unit conversion from meter to kilometer

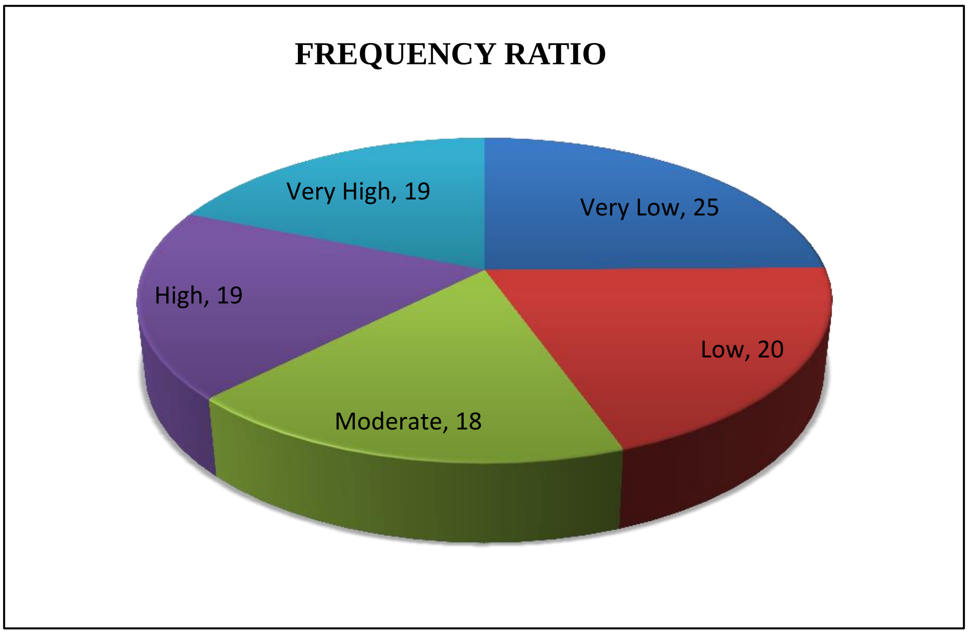

Figure 4.7 Distribution of landslide susceptibility classes of frequency ratio in the study area

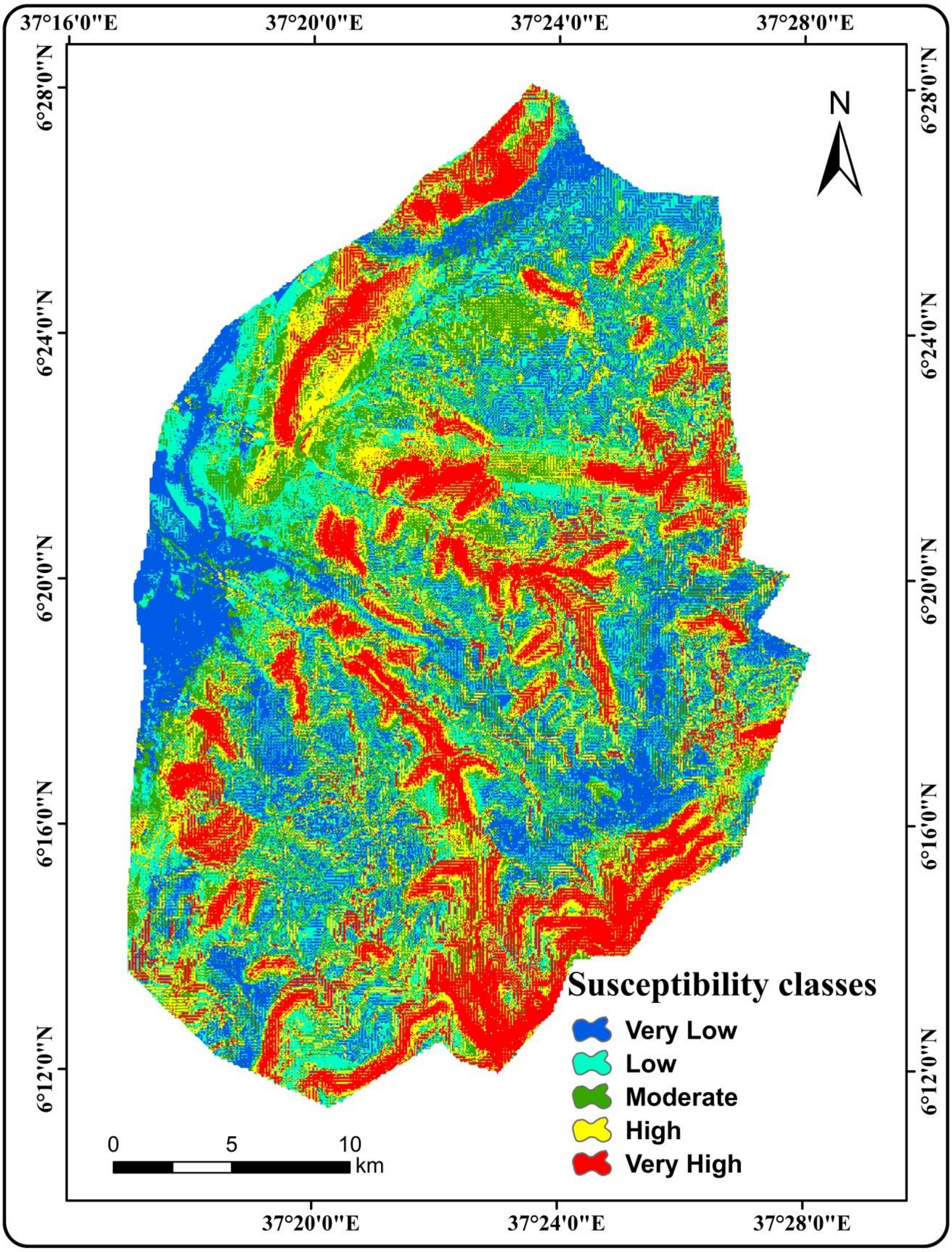

Figure 4.8 Landslide Susceptibility map using frequency ratio

4.5 Results of Analytical Hierarchy Process Model

4.5.1 Relationship between landslide and causative factors

As indicated in Table 6 and Figure 4.9, slope was the major parameter contributing to the landslide of the study area with a relative weight of 27.3%, followed by aspect, curvature, LULC, NDVI, lithology, and distance to the road of 18.2%, 15.1%, 10.8%, 8.5%, 6.7%, and 5.1% relative weight, respectively, whereas distance to the fault, distance to the stream, and distance to the lineament have a lower contribution to landslide occurrence with a relative weight of 3.9%, 2.9%, and 1.6%, respectively. The area is characterized mainly by a moderately to very steep slope or cliff, highly weathered rhyolite and highly weathered basalt, quaternary deposits, and also by aspect, curvature, LULC, NDVI, and distance to the road. Distance to the fault, distance to the stream, and distance to the lineament are the next influential parameters, with more or less equal influences on landslide occurrences.

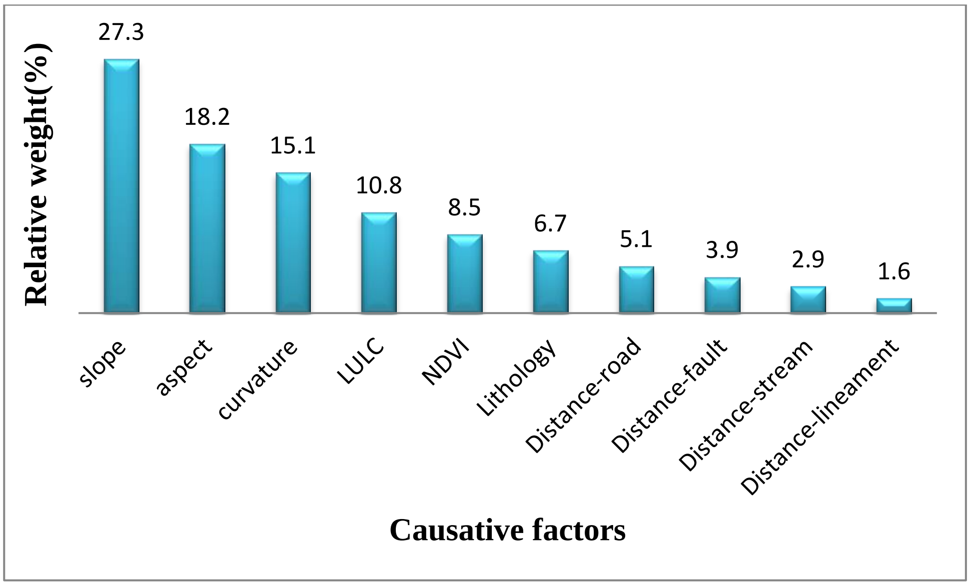

Figure 4.9 Relationship of landslide occurrence with the causative factors of analytical hierarchy process

4.5.2 Rating Landslide Factors using analytical hierarchy process

All ten factors play a role in landslide occurrence, but their individual contributions to slope instability vary significantly. This classification process involved the prioritization and weighting of field-based expert judgment and the review of published data (Abay and Barbieri, 2012). Each pair of factors was assigned a value between 9 (extremely influential) and 1/9 (oppositely influential), using a scale derived from Table 2. These values formed a square reciprocal matrix (Table 6) by rating rows relative to columns. Then after the judgmental matrix resulting from pair wise comparisons was subjected to consistency checks to ensure the validity of the results. Quantifying the relative importance of the landslide causative factors involved constructing a pair wise comparison and judgment matrix, as guided by Saaty's (1980, 2000). The numerical relational scale from Table 2 was employed for comparing pairs of attributes (parameters within a layer). To check for consistency in the results, two values were calculated: the consistency index (CI) using equation 6, and the consistency ratio (CR) using equation 7. A reference value, called the random consistency index (RI), was also used from Table 1. For this analysis with ten factors, the RI was 1.49.

The consistency ratio (CR) serves as a measure of agreement within the judgments made in a pair wise comparison matrix. A CR value of 10% or less indicates acceptable consistency, while values exceeding 10% suggest potential inconsistencies. In this study, the calculated CR for the study area derived using equation (7) and the data in Appendices II–IV was 9.55%. This falls within the acceptable range, confirming the consistency of the judgments made in the matrix.

Table 6 pair-wise comparisons for all landslide causative factors

factor	slope	aspect	curvature	LULC	NDVI	Lithology	Distance-road	Distance-fault	Distance-stream	Distance-lineament	Relative weight (%)
slope	1	3	4	3	3	5	5	8	6	9	27.3
aspect	0.33	1	3	3	4	4	3	5	4	7	18.2
curvature	0.25	0.33	1	3	3	5	3	5	7	5	15.1
LULC	0.33	0.33	0.33	1	3	3	3	3	3	8	10.8
NDVI	0.33	0.25	0.33	0.33	1	3	3	3	3	6	8.5
Lithology	0.2	0.25	0.2	0.33	0.33	1	3	3	3	7	6.7
Distance-road	0.2	0.33	0.33	0.33	0.33	0.33	1	3	3	3	5.1
Distance-fault	0.125	0.2	0.2	0.33	0.33	0.33	0.33	1	3	5	3.9
Distance-stream	0.167	0.25	0.14	0.33	0.33	0.33	0.33	0.33	1	3	2.9
Distance-lineament	0.111	0.143	0.2	0.125	0.167	0.143	0.33	0.2	0.33	1	1.6

4.5.3 Landslide Susceptibility mapping using analytical hierarchy process approach

In this study, the landslide susceptibility maps were quantitatively prepared using the analytical hierarchy process in a GIS environment. Weight of each causative factor class was defined by the combination of each parameter and landslide inventory map. By combination of following decision rules (addition, division, multiplication, and subtraction), the weight of each conditioning factor class was defined. Finally, the landslide susceptibility index classification using the natural breaks method was done as it is well suited to evenly distributed data.

From the weight sum, the final result of LSI values of the study area ranges from 0.508 to 1.676. The LSI map was classified into five classes using the natural breaks method this method is used because it is best for uneven data distribution, and it is capable of classifying the landslide susceptibility index map into a different category based on the inherent data value similarity (Meten et al., 2015). Therefore, the LSI values were classified into five susceptibility areas: very low (0.508 – 0.634), low (0.634 – 0.707), moderate (0.707 – 0.808), high (0.808 – 0.961) and very high (0.961 – 1.676) [Table 7].

Table 7 Analytical hierarchy process Landslide susceptibility class based on landslide susceptibility index

Susceptibility classes	LSI	Area (km^2)	Area (%)
Very Low	0.508 – 0.634	13.13	3
Low	0.634 – 0.707	33. 67	7
Moderate	0.707 – 0.808	112.48	26
High	0.808 – 0.961	157.40	36
Very High	0.961 – 1.676	121.15	28

The landslide susceptibility map (Figure 4.11 and Table 7) clearly shows that in the study area, 13.13km^2 (3%) falls in very low susceptible classes and 121.15km^2 (28%) of the area falls in very high susceptibility classes while the remaining ones including 33.67km^2 (7%), 112.48km^2 (26%), and 157.40km^2 (36%) of the study area fall in low, moderate and high susceptibility classes respectively, were estimated from the ratio of the product of pixels and 30m*30m cell size to 10^6. Where 10^6 is the unit conversion from meter to kilometer

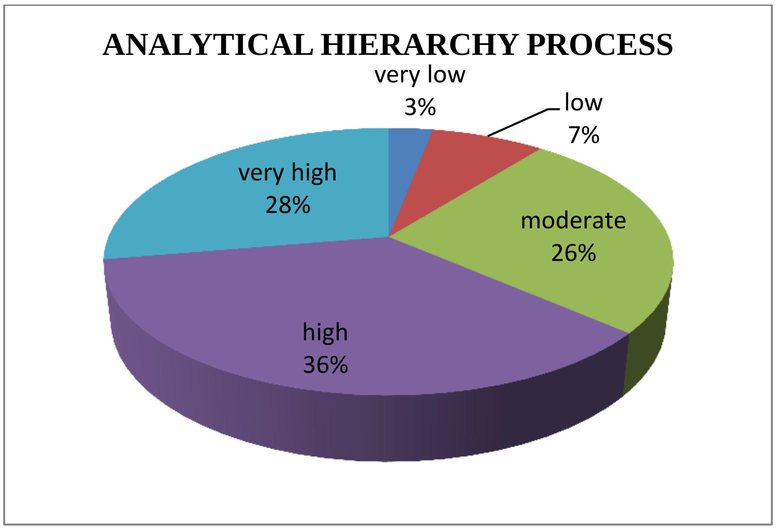

Figure 4.10 Distribution of landslide susceptibility classes of analytical hierarchy process in the study area

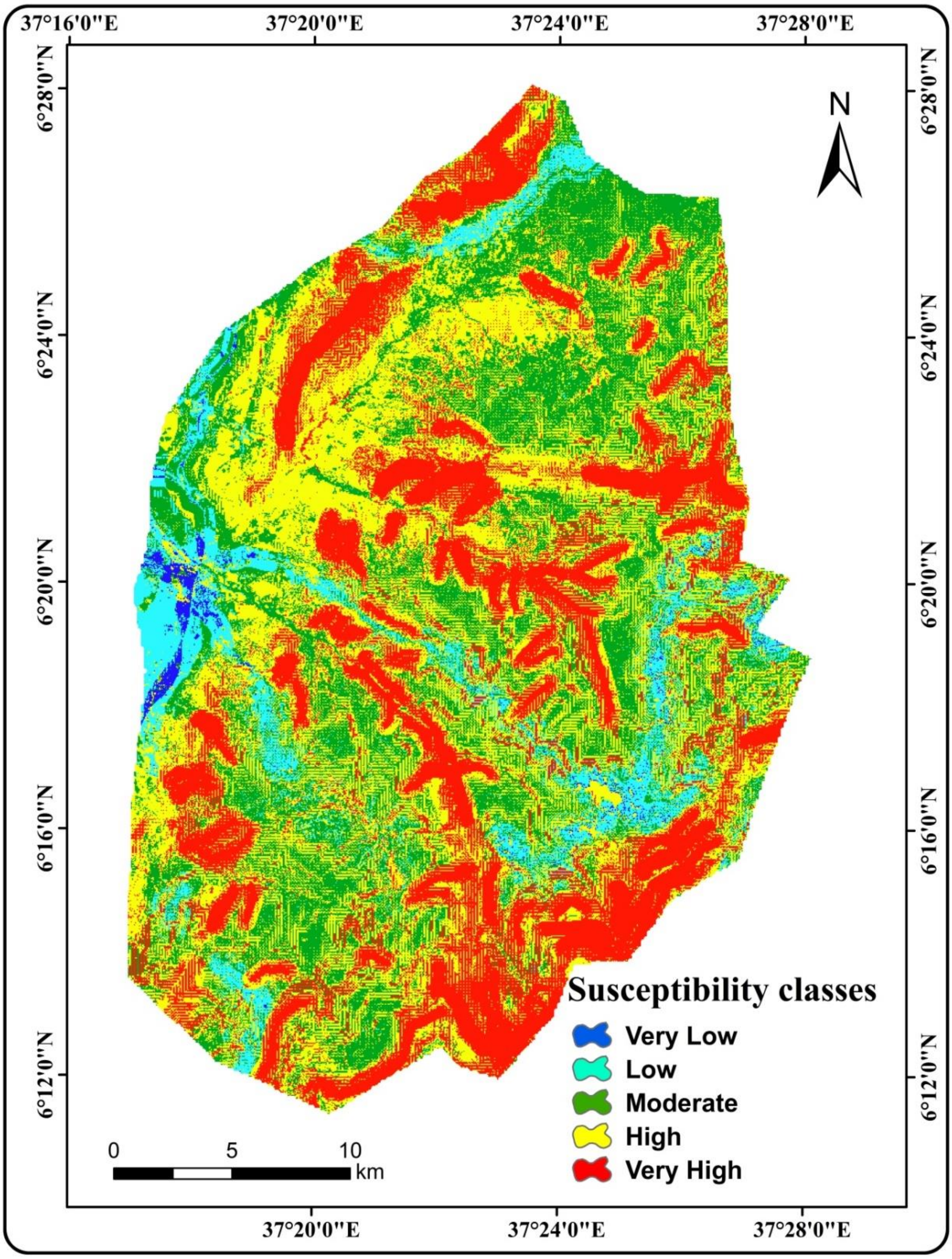

Figure 4.11 Landslide Susceptibility map using analytical hierarchy process

Assessment of the developed map indicated that the terrain and plateau part of the study area, including the localities of Ako, Menena, Degeza, Zongala, Alaha, Wulokode showed very high and high susceptibility classes. Localities of Wacha, Shella Subo, Gebeko, Halaha and Selam fall in very low, low and moderate susceptibility classes. In general, most of the South, southeast, northeast, north and middle part of the study area falls under high and very high susceptibility zones. Very low, low, and moderate susceptibility classes are distributed throughout the study area.

4.6 Model validations

In this study, the combination of the landslide susceptibility and landslide inventory map is typically used to determine the quality of a landslide susceptibility model. Out of the 793 landslides found, 555 (70%) were used to create the landslide susceptibility maps, and 238(30%) were used to test the model. Both the analytical hierarchy process and the frequency ratio approach were used to investigate the landslide susceptibility.

For validation, the area under the curves (predictive and success rates) was used by using the 30% validation landslides in both landslide susceptibility maps. The success rate was estimated by comparing the training data set with the landslide susceptibility class, whereas the predictive rate was calculated by comparing the validation data set with landslide susceptibility classes.

4.6.1 Area under the Curve (AUC) Success and Predictive Rate Curve

The results showed that the AUC of the success rate of frequency ratio was 0.873 and the predictive rate was 0.810. The AUC of the success rate and predictive rate curves ranges between 0.8 and 0.9, indicating very good performance of the landslide susceptibility models. Based on the AUC evaluation, the landslide susceptibility maps produced by the models were reliable

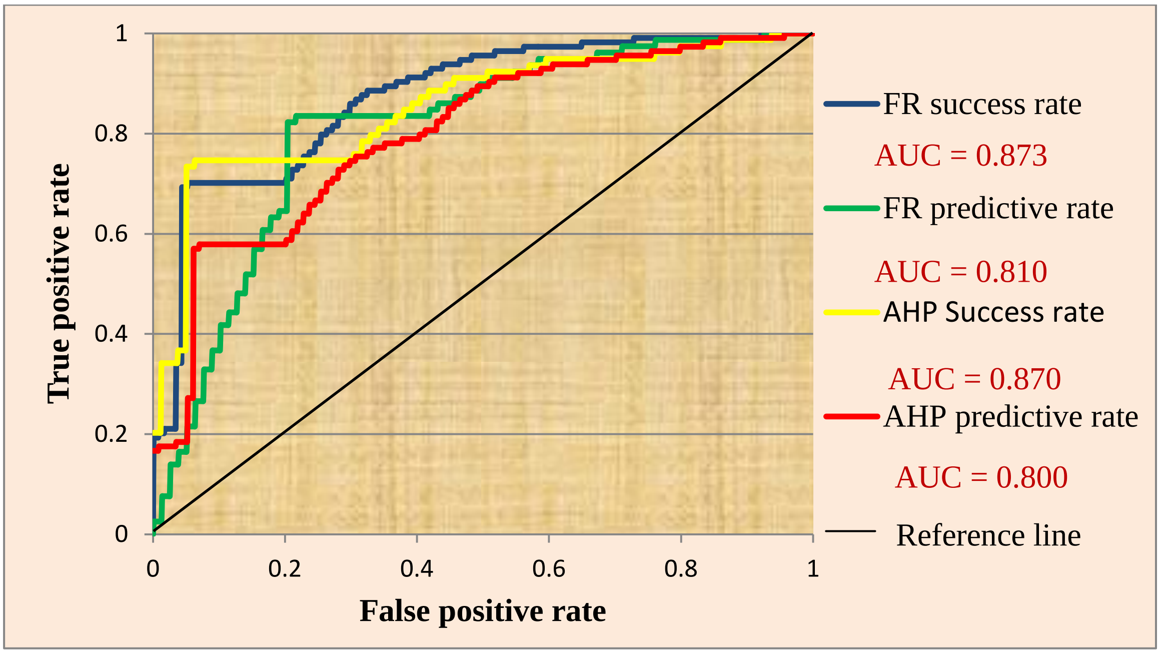

Figure 4.12 Success and predictive rate of frequency ratio analytical hierarchy process approach

4.7 Remedial measures

Increasing Vegetation Cover

In the study area, the susceptibility classes of both the AHP and FR approaches were categorized into moderate, high, and very high probability for landslide occurrence. The AHP approach indicated that 36% of the area falls in the moderate susceptibility class, 26% in the high susceptibility class, and 28% in the very high susceptibility class. On the other hand, the FR approach showed that 18% of the area is in the moderate susceptibility class, 18% in the high susceptibility class, and 19% in the very high susceptibility class. These results were validated field observation of landslide susceptible area those need remedial. To prevent landslide hazards in the area, planting vegetation on hillsides is a very economical and effective way to ensure the stability of slopes, as it helps to bind the soil together and prevent excessive run-off and soil erosion.

Surface Drainage Work

The drainage system is practically zero on the vulnerable slopes of the study area, particularly Menena, Zongala, and Wulokode. This leaves them exposed to the dangers of rainwater infiltration and flooding, ultimately jeopardizing their stability. But providing surface drainage works is recommended specifically for areas prone to floods and seasonal streams.

Retaining wall construction

Gully and stream bank erosion pose a serious threat to the stability of several areas in your study area, notably Dida, Ako, Degeza, Alaha and Menena. Especially during the rainy season, these waterways can unleash powerful erosive forces, leading to land loss and potentially triggering slope instability. But there are Proactive measures like **r**etaining walls and gabion walls can be vital allies in the fight against erosion.

Public awareness and education plan

Understanding landslide threats is the first step towards mitigating their impact. Widespread public awareness empowers individuals and communities to make informed decisions about where they live, work, and cultivate land. With knowledge readily available, communities can actively plan, mitigate risks, and prepare for landslides, building rnesilience and reducing their vulnerability to these earth-moving events.

5. CONCLUSIONS AND RECOMMENDATIONS

5.1 Conclusions

A landslide susceptibility assessment was used as input in the analysis of landslide risk and hazards. A frequency ratio and an analytical hierarchy process approach were used to assess the spatial probability of a landslide occurrence in this study. The landslide inventory of the study, identified through Google Earth Pro and field surveys, was a total of 793 landslides. These landslides include debris slides, rotational and translational slides, progressive creep movement, rock slides, rock falls, and complex types of landslides. These landslide inventories were partitioned into a training dataset of 70% (555), which was used for the statistical application, and a validation dataset of 30% (238), which was used to evaluate the performance of the models used.

This study considered ten causative factors in preparing the landslide susceptibility maps. These were included: slope, aspect, curvature, lithology, land use/land covers, normalized difference vegetation index, distance to road, distance to fault, distance to streams, and distance to lineaments. Their thematic maps were prepared: slope, aspect, curvature, and distance to stream were prepared from the SRTM DEM with a 30m*30m resolution; land use, land cover, and NDVI were prepared from Sentinel 2A; and lineament maps were prepared from the Google Earth image of 2023 and field survey in the ArcGIS environment. The lithology and distance to fault map layers of the study area were extracted from the geological maps of Dime with a scale of 1:250,000 and a field survey. Rainfall data was generated from the rain-fall data of the National Meteorological Agency of Ethiopia. Later, all vector maps were transformed into raster data of the same cell size for further analysis.

To identify the spatial relationship between the occurrence of landslides and each landslide's causative factor classes, causative factor maps were combined with a training data set to get each class’s weight. In the present study, the contribution of landslide occurrence to each causative factor class was identified by statistical frequency ratios and analytical hierarchy process values. From the frequency ratio analysis, FR values greater than 1 were found in the factor class of a slope greater than 28°: concave and convex curvatures; aspect classes of north, west, southwest, northeast, and southeast facing slopes; lithology of basalt; land use and land cover of sparse forest, bare land, and shrubs; normalized difference vegetation index of _0.120 - 0.144, 0.144 - 0.200, and 0.200 - 0.269; distance to road of 0 -100m, 100 - 200m, 200 - 300m, and 300 - 400m; distance to fault of 0 -100m, 100 - 200m, 200 - 300m, 300 - 400m, 400 -500m and 500 - 600m; distance to stream of 0 -100m, 100 - 200m, 200 - 300m, 300 - 400m, 400 -500m and 500 - 600m; distance to lineament of 0 - 50m, 50 - 100m, 100 -150m, 150 - 200m, 200 - 250m, and 250 - 300m that had highest probability of landslide occurrence. Whereas FR values less than 1 of the factor classes indicated a lower probability of landslide occurrence. The analysis of the analytical hierarchy process approaches the value of the area where there is a high relationship if the relative weight is high; otherwise, there is a low relationship. As a result, slope had the highest probability of landslide occurrence, followed by aspect, curvature, LULC, NDVI, lithology, and distance to the road, whereas distance to the fault, distance to the stream, and distance to the lineament had a lower contribution to landslide occurrence. Finally, the landslide susceptibility index of both models was subdivided into very low, low, moderate, high, and very high susceptibility classes.

The quality of the proposed models was validated using AUC for the accuracy assessment of the resulting landslide susceptibility maps. The model was created using a dataset of past landslides (the training set), and the model was then tested on a different dataset of landslides that the model had never seen before (the validation set). The model performed well on both the training and validation sets, indicating that it can accurately predict landslides in new areas. In this study, the AUC of the success rate and predictive rate curves ranged between 0.8 and 0.9, indicating the good performance of both methods. The FR and AHP approaches were validated using the ROC curve. The AUC values for both approaches were high, indicating that they are both accurate in predicting landslide susceptibility. The success rate for the FR approach was 0.873, while the success rate for the AHP approach was 0.87. The predictive rate for the FR approach was 0.81, while the predictive rate for the AHP approach was 0.80. The results and findings of this study can help developers, planners, and engineers identify areas that are susceptible to future hazards.

Based on the results obtained from landslide susceptibility maps, effective and economical remedial measures can be recommended for moderate, high, and very high susceptibility zones in the study area. These remedial measures included the construction of retain walls, drainage system work, vegetation covers, and public awareness and education.

.

5.2. Recommendation

Landslides are caused by complex interactions in the natural environment, and these interactions can be further complicated by human activities. To reduce losses from landslide hazards, sustained and long-term efforts are needed. Landslides in the study area are caused by both natural and human factors. Natural factors include intense and prolonged rainfall, steep slopes, erosion, and shallow groundwater. Human factors include deforestation and the construction of roads and houses in hazardous areas. Landslides in the study area have caused significant damage to the environment, agricultural land, roads, and houses. To reduce landslide hazards in the study area, it is important to:

Reduce deforestation: Trees help to hold the soil in place, so reducing deforestation can help to prevent landslides.

Avoid building in hazardous areas: Areas that are steep, unstable, or have a history of landslides should be avoided for development.

Improved drainage: Proper drainage can help prevent water from saturating the soil and triggering landslides.

Educate the public: Educating the public about landslide hazards and how to reduce their risk is important for reducing losses from landslides.

By taking these steps, we can help reduce the risk of landslides and protect people and property in the study area.

References

Addis, Abinet. (2022). Landslide Susceptibility Mapping Using GIS and Bivariate Statistical Models in Chemoga Watershade , Ethiopia. 1–21.

Addis, Abinet. (2023). GIS-Based Landslide Susceptibility Mapping Using Frequency Ratio and Shannon Entropy Models in Dejen District, Northwestern Ethiopia. Journal of Engineering (United Kingdom), 2023, 25–29.https://doi.org/10.1155/2023/1062388

Aipe, E. and Sailesh, M. (2016). Landslide vulnerability mapping (LVM) using weighted linear combination (WLC) model through remote sensing and GIS techniques. Modeling Earth Systems and Environment, 2(2), 1–15. https://doi.org/10.1007/s40808-016-0141-7

Aleotti, P and Chowdhury, R. (1999). Landslide hazard assessment: summary review and new perspectives. Bull. Int. Assoc. Eng. Geol, 58, 21–44.

Anbalagan, R. (1992). Landslide hazard evaluation and zonation mapping in mountainous terrain. Eng. Geol.32: 269-277

Anis, Z, Wissem, G, Vali, V, Smida, H. and Mohamed Essghaier, G. (2019). GIS-based landslide susceptibility mapping using bivariate statistical methods in North-western Tunisia. Open Geosciences, 11(1), 708–726. https://doi.org/10.1515/geo-2019-0056

Ayalew, Lulseged. (1999). The effect of seasonal rainfall on landslides in the highlands of Ethiopia. Bulletin of Engineering Geology and the Environment, 58(1), 9–19. https://doi.org/10.1007/s100640050065.

Ayalew, Lulseged and Yamagishi, Hiromitsu. (2004). Slope movements in the Blue Nile basin, as seen from landscape evolution perspective. Geomorphology 57:97–116.

Ayalew, Lulseged and Yamagishi, Hiromitsu. (2005). The application of GIS-based logistic regression for landslide susceptibility mapping in the Kakuda-Yahiko Mountains , Central Japan. 65, 15–31.https://doi.org/10.1016/j.geomorph.2004.06.010

Ayalew, Lulseged and Yamagishi, Hiromitsu. (2005). Inventory of landslides and susceptibility mapping in the Dessie area, Northern Ethiopia. Eng Geol 77:1–15.

Berhane, Gebremedhin and Tadesse, Kumarra. (2021). Journal of African Earth Sciences Landslide susceptibility zonation mapping using statistical index and landslide susceptibility analysis methods : A case study from Gindeberet district , Oromia Regional State , Central Ethiopia. Journal of African Earth Sciences, 180, 104240.

https://doi.org/10.1016/j.jafrearsci.2021.104240.

Beyth M. (1972). Paleozoic-Mesozoic sedimentary basin of Mekele Outlier, Northern Ethiopia.American Association Petroleum Geologists Bulletin.56:2426- 2439.

Beza, Yechale. (2021). GIS-Based Statistical Analysis for Evaluation of Landslide Susceptibility Mapping: A Case Study in Blue Nile Gorge, Gohatsion-Dejen Road Section, Central Ethiopia.

Carrara, A, Cardinali, M. and Guzzetti, F. (1992). Uncertainty in assessing landslide hazard and risk. ITCJ. 2:172–183.

Cheng Su, Lili Wang, Xizhi Wang, Zhicai Huang and Xiaocan Zhang. (2015). Mapping of rainfall-induced landslide susceptibility in Wencheng, China, using support vector machine. Natural Hazards.Volume.76, pages1759–1779

Che, V. B., Kervyn, M., Ernst, G. G. J., Trefois, P., Ayonghe, S., Jacobs, P., Ranst, E. Van, and Suh, C. E. (2011). Systematic documentation of landslide events in Limbe. 47–74. https://doi.org/10.1007/s11069-011-9738-3

Corominas, J. and Mavrouli, O. (2011). Living with landslide risk in Europe: Assessment,effects of global change, and risk management strategies. SafeLand ;Guidelines for landslide susceptibility, hazard and risk zoning , 1-173.

Corominas, J. and Mavrouli, O. (2023). Quantitative risk assessmenent for buildings due to rock- falls : some achievements and challenges Quantitative risk assessmenent for buildings due to rock- falls : some achievements and challenges. August 2015.

Dai, F.C. and Lee, C.F. (2001). Terrain-based mapping of landslide susceptibility using a geographical information system: a case study. Can. Geotech. J. 38: 911–923.

Dai, F.C., Lee, C.F. and Ngai, Y.Y. (2002). Landslide risk assessment and management: an overview. Eng. Geol. 64: 65–87

Fall, M., Azzam, R and Noubactep, C.(2006).A multi-method approach to study the stability of natural slopes and landslide susceptibility mapping. Eng. Geol. 82: 241–263

Fell, R., Corominas, J., Bonnard, C., Cascini, L., Leroi, E., and Savage, W. Z. (2008). Guidelines for landslide susceptibility , hazard and risk zoning for land use planning. Engineering Geology, 102(3–4), 85–98. https://doi.org/10.1016/j.enggeo.2008.03.022

Firomsa, Misgana and Abay, Asmelash. (2019). Landslide assessment and susceptibility zonation in Ebantu district of Oromia region , western Ethiopia. 4229–4239.

Genene, Alembante. and Meten, Matebie. (2021). Landslide Susceptibility Mapping Using GIS-based Information Value and Frequency Ratio Methods in Gindeberet area, West Shewa Zone, Oromia Region, Ethiopia. http://dx.doi.org/10.21203/rs.3.rs-219331/v1

Getachew, Nega. and Meten, Matebie. (2021). Weights of evidence modeling for landslide susceptibility mapping of Kabi-Gebro locality , Gundomeskel area , Central Ethiopia.

Gomez H, and Kavzoglu T. (2005). Assessment of shallow landslide susceptibility using artificial neural networks in Jabonosa River Basin, Venezuela. J EngGeol 78(1–2):11–27.

Glade, T. (2003). Landslide occurrence as a response to land use change : a review of evidence from New Zealand. 51, 297–314.

Greenway, D.R. (1987). Vegetation and slope stability. In Slope Stability, Anderson MG, Richards KS (eds.). John Wiley: Chichester; pp.187-230.

Guzzetti F, Mondini AC, Cardinali M, Fiorucci F, Santangelo M, Chang KT. (2012). Landslide inventory maps: new tools for an old problem. Earth-Sci Rev 112(1):42–66

Hungr, O., Leroueil, S and Picarelli, L. (2014). The Varnes classification of landslide types, an update. Landslides, 11(2), 167-194

Highland, L.M. and Bobrowsky, P. (2008).The Landslide Handbook- A Guide to Understanding Landslides. U.S. Geological Survey, Reston, Virginia, 147 pp

Hyun-Joo , Saro Lee, Wisut Chotikasathien, C. H. and J. H. (2009). Predictive landslide Thailand, susceptibility mapping using spatial information in the Pechabun area of Environmental. Geology, 57, 641–651.

Ishizaka, A and Labib, A. (2009).Acomparative Study of conventional, ANN black box, fuzzy and combined neutral and fuzzy weighting procedures for landslide susceptibility Zonation in Darjeeling Himalayas. Engineering geology, 85. Pp 347-366

Kanungo D.P., Arora, M.K., Sarkar, S. and Gupta, R. (2006). Landslide susceptibility zonation mapping a review. J South Asia Disaster Stud, 2, 81 – 105.

Kanungo D.P., Arora, M.K., Sarkar, S. and Gupta, R. (2009). Landslide susceptibility zonation mapping a review. J South Asia Disaster Stud, 2, 81 – 105.

Katzmin, V. (1972). Geological Map of Ethiopia. EIGS, Addis Ababa

Khan, H, Shafique, M, Khan, M, Bacha, M, Shah, S, and Calligaris, C. (2019). Landslide susceptibility assessment using Frequency Ratio, a case study of northern Pakistan. The Egyptian Journal of Remote Sensing and Space Science, 22(1), 11-24. Doi: 10.1016/j.ejrs.2018.03.004

Komac M. (2006). A landslide susceptibility model using the analytical hierarchy process method and multivariate statistics in perialpine Slovenia. Geomorphology 74(1–4):17–2.

Kumar, T, Negassa, L, and Kala, P. M. (2015). GIS based Grid overlay method versus modeling approach – A comparative study for landslide hazard zonation (LHZ) in Meta Robi District of West Showa Zone in Ethiopia. The Egyptian Journal of Remote Sensing and Space Sciences, 18(2), 235–250. https://doi.org/10.1016/j.ejrs.2015.08.001

Lee, S. and Pradhan, B. (2007). Landslide hazard mapping at Selangor, Malaysia using frequency ratio and logistic regression models. Landslides, 4:33–41.

Leroi, E. (1997). Landslide risk mapping: problems, limitation and developments inCruden, Fell (Ed.), Landslide Risk Assessment. Balkema, Rotterdam, pp. 239–250

Li SZ, Dai S, Wang HW and Zhang X .(2015). Fault features and their implications on distribution and formation of landslides in Bailongjiang Region. Journal of Lanzhou University (Natural Sciences) 51(2): 145-152 (In Chinese)

Marden, M, Phillips, C. J, Jackson, R. J, Zhang, X. B. and Ekanayake, J. (1992). Landslide hazard mapping at Selangor, Malaysia using frequency ratio and logistic regression models. Landslides, 4:33–41.

Michael, E. A, and Samanta, S. (2016). Landslide vulnerability mapping (LVM) using weighted linear combination (WLC) model through remote sensing and GIS techniques. Environmental Earth Sciences. https://doi.org/10.1007/s12665-015-4377

Merla,G., Abbate,E, Azzoroli,A.,Bruni,P.,Canuti,P.,Fazzuoli,M.Sagri,M and Tacconi, P. (1979). A Geological map of Ethiopia and Somali, CNR, Italy.

Meten, Matebie. (2015). Application of GIS-based fuzzy logic and rock engineering system (RES) approaches for landslide susceptibility mapping in Selelkula area of the Lower Jema River Gorge , Central Ethiopia. Environmental Earth Sciences. https://doi.org/10.1007/s12665-015-4377-8

Mersha, Tilahun, and Meten, Matebie. (2020). GIS-based landslide susceptibility mapping and assessment using bivariate statistical methods in Simada area , northwestern.

Musinguzi, M, and Asiimwe, I. (2014). Application of Geospatial Tools for Landslide Hazard Assessment For Uganda. South African Journal of Geomatics, Vol. 3, , (No. 3), 302314. doi:DOI: http://dx.doi.org/10.4314/sajg.v3i3.4

Necdet, T. (2011). Computers & Geosciences Mapping erosion susceptibility by a multivariate statistical method : A case study from the Ayvalık region , NW Turkey. 37, 1515–1524. https://doi.org/10.1016/j.cageo.2010.09.006

Nelson, S. (2010). Slope stability, Triggering events, Mass wasting hazards. https://doi.org/10.1007/s11069-006-9030-0

O' Loughlin, C. (2005).The protective role of trees in soil conservation, feature: land use impacts. Journal of forestry. Pp 9-15.

Pardeshi SD, Autade SE, and Pardeshi. (2013). Landslide hazard assessment: recent trends and techniques. Springer, 2:1–11.

Pham, B. T., Tien Bui, D., Indra, P., and Dholakia, M. (2015).Landslide susceptibility assessment at a part of Uttarakhand Himalaya, India using GIS-based statistical approach of frequency ratio method. Int J Eng Res Technol, 4(11), 338-344.

Pradhan, B. and S. Lee. (2006). Probabilistic landslide hazards and risk mapping on Penang Island Malaysia. Earth System Science, 115, 661–672.

Prandini, L., Guidicini, G., Bottura, J.A., Poncano, W.L and Santos, A.R. (1977). Behavior of the Vegetation in Slope Stability: A Critical Review. Bull. IAEG, 16: 51-55.

Raghuvanshi, T.K, Jemal Ibrahim and Dereje Ayalew (2014a).Slope stability susceptibility evaluation parameter (SSEP) rating scheme – an approach for landslide hazard zonation. J. Afr. Earth Sci. 99: 595–612.

Raghuvanshji, T.K, P.M. Kala and M. Singh (2014 b). Landslide disaster management and reduction-An approach through remote sensing and Gis. In: Landscape Ecology and Water Management, proceeding of International Geographical Union (IGU) Rohatic

Conference, Advance in Geographical and Enviromental Science(M.singh,R.B. Singh and M.I. Hassen:Editor), Sringer Japan. Vol_2,pp.33-40.

Raghuvanshi, T. K., Negassa, L., and Kala, P. M. (2015). GIS based Grid overlay method versus modeling approach–A comparative study for landslide hazard zonation (LHZ) in Meta Robi District of West Showa Zone in Ethiopia. The Egyptian Journal of Remote Sensing and Space Science, 18(2), 235-250.

Saaty, T.L. (1980). The Analytic Hierarchy Process: Planning, Priority Setting, Resource Allocation. 2nd edition, McGraw-Hill International Co., ISBN: 9780070543713, 287p.

Saaty, T.L. (2000). The fundamentals of decision making and priority theory with the analytic hierarchy process.2nd edition, RWS Publications, Pittsburg, 478p.

Saaty TL, Vargas LG. (2006). Decision making with the analytic network process:economic, political, social and technological applications with benefits, Opportunities, Costs and Risks. Springer, New York.

Saaty T. (2008). Decision making with the analytical hierarchy process: Int JServices Sci 1(1):83–98.

Shah, S., D. and Nagarajan, R. (2004). Geological, Structural and ectonics aspects of Landslides: Landslide Disaster assessment and Monitoring. Nagarajan R.Anmol Publication.Pp 22-36.

Sharma, L. P., Patel, N., Debnath, P., and Ghose, M. K. (2012). Assessing landslide vulnerability from soil characteristics—a GIS-based analysis. Saudi Society for Geosciences-Springer, 789–796.

Sideng, Uca and Maru, Rosmini and Nyompa, Sukri and Arfan, Amal and Malik, Abdul and Abidin, M. R. (2018). Mapping and Zonation Level of Landslides Hazard and Risk Assessment: A Case Study of Enrekang Regency, South Sulawesi, Indonesia. Thai Society of Higher Education Institutes on Environment, 11 (2). pp. 149-163.

Tefera, M, Chernet, T, and Haro, W. (1996). Explanation of the Geological Map of Ethiopia, second ed. EIGS, Addis Ababa

Woldearegay, K. (2008). Characteristics of a large-scale landslide triggered by heavy rainfall in Tarmaber area, central highlands of Ethiopia. Geophys Res Abstr 10 : EGU2008-A-04506 2008, SRef–ID:16077962/gra/EGU2008-A-04506.

Woldearegay, K. (2013a). Review of the occurrences and influencing factors of landslides in the highlands of Ethiopia : With implications for infrastructural development. 5(1996), 3–31.

Wubalem, A. (2021). Landslide susceptibility mapping using statistical methods in Uatzau catchment area , northwestern Ethiopia. 1–21.

USG. (2004). www.pubs.usgs.gov/fs/2004/3072/pdf/ fs2004-3072.pdf: accessed on April, 17, 2020.

Van Westen, C.J., Rengers, N. and Terlien, M.T.J. (1997). Prediction of the occurrence of slopeinstability phenomena through GIS-based hazard zonation. Geol. Rundsch, 86: 4004– 4414.

van Westen, C. J., van Asch, T. W. J., and Soeters, R. (2006). Landslide hazard and risk zonation .Bulletin of Engineering Geology and the Environment, 65(2), 167–184. https://doi.org/10.1007/s10064-005-0023-0

Varnes, D.J. (1978). Slope movement types and processes. In: Schuster RL, Krizek RJ (eds.), Landslides: Analysis and Control. National Academy of Sciences, Transportation Research Board, Washington DC, Special Report 176, 11-35.

Varnes D. J.(1984).Landslide Hazard Zonation: A review of principles and practices. UNESCO, Paris. pp. 1-63.

Voogd H. (1983). Multicriteria evaluation for urban and regional planning. Pion Ltd., Londo

Xu, C., Dai, F., Xu, X., and Lee, Y. H. (2012). GIS-based support vector machine modeling of earthquake-triggered landslide susceptibility in the Jianjiang River watershed, China. Geomorphology, 145–146, 70–80. https://doi.org/10.1016/j.geomorph.2011.12.040

Yalcin, A., and Bulut, F. (2007). Landslide susceptibility mapping using GIS and digital photogrammetric techniques : a case study from Ardesen. 201–226. https://doi.org/10.1007/s11069-006-9030-0

Zahedi, F. (1986). The analytic hierarchy process, a survey of the method and its applications. Interfaces, 16(4):96-108.

APPENDIX

Appendix I Precipitations of three stations (29yr); Arbaminch, Dara malo and Chancho stations in millimeter.

Station	years	Jan	Feb	Mar	Apr	May	Jun	Jul	Aug	Sep	Oct	Nov	Dec	Annual Rainfall
Arbaminch	1992	12.8	18.1	27.1	164.8	140.2	131.9	32	42.8	132.2	172.7	59.6	29.3	963.50
	1993	178	120.8	34.4	94.8	198.2	52.6	3.1	24.6	31.4	117.1	18.2	1.2	874.40
	1994	0.3	4.1	36.4	183.9	164.6	59.9	72.1	82.9	29.7	70.3	59.6	18.8	782.60
	1995	0.4	27.1	54.4	256.8	140.4	85.3	21.6	17.6	84.7	109.1	53.6	43.5	894.50
	1996	0.4	32.7	52.9	283.3	123.9	90.4	23.4	20.1	100.6	117.4	58.3	29	932.40
	1997	16	0.4	18	240.8	172.5	27.7	61	27.8	49.1	214.6	273.1	152.8	1253.80
	1998	66.6	90.1	24.3	165.8	96.5	41.2	30.4	28.2	42	148.5	58.5	0.8	792.90
	1999	17.1	0.7	109	136.9	43.2	44.2	79.2	23.9	68.9	203.6	9.7	44.5	780.90
	2000	1.3	0	19.3	92.4	236.1	40.7	61.7	39.1	70.4	185.8	56	65.8	868.60
	2001	68.7	86.6	56	175.3	236.3	52.9	40.7	45.1	108.2	123.9	85.1	5.5	1084.30
	2002	42.9	22.4	93.9	112.4	56.5	52.2	55.1	12.4	87.9	87.7	18.1	167.2	808.70
	2003	13.5	11.3	61.6	201.1	192.1	98.1	30.2	105.5	39.6	89.4	25.8	14.2	882.40
	2004	41.7	31.2	17.5	164.8	58.7	34.8	22.2	69.9	81.6	60.9	143	32	758.30
	2005	29	1.4	67.1	311.1	221.4	16.3	28.8	22.3	77.4	120.6	33.4	4.3	933.10
	2006	12.8	83.9	137.4	115.4	129.7	126.2	24.4	75.2	42.8	158.7	103.3	118.6	1128.40
	2007	63.4	35.5	16.9	129.4	193.4	107.2	111.8	99.3	246.4	76.3	61.5	0	1141.10
	2008	0.6	9	60.1	135.1	48.4	76	33.8	56	200.8	149	81.7	0	850.50
	2009	45.1	3.1	28.5	98.5	109.4	14.9	1.4	16.2	41.3	162.2	14.1	104	638.70
	2010	19.2	49.7	191	177.9	222.2	80.7	39.7	33.7	146.1	95.1	4.5	8.3	1068.10
	2011	0	28.6	18.9	30.7	257.5	60.8	28.1	84.7	154.8	73.8	256.8	11.6	1006.30
	2012	0	2.2	30.5	319.7	67.9	72.3	28.2	57	193	129.7	79.3	33.6	1013.40
	2013	27.4	6.9	87.7	240.9	111.1	87.8	48.6	33	78.4	245	86.6	7.7	1061.10
	2014	8.7	44.3	71.2	70.3	208.4	73.1	15.1	77	105.2	132.2	59.3	1.4	866.20
	2015	0	2.7	57.1	122.4	177.5	131.7	19.4	18.8	64.6	202.4	209.4	115.3	1121.30
	2016	3.4	9.4	39.1	263.1	66.3	111	7.9	51.7	25.2	118.1	95.6	4.3	795.10
	2017	0.6	28.5	18.6	91.2	188.3	2.7	27.4	120.8	92.6	111.6	70.3	0	752.60
	2018	0	47.6	35.5	220	135.6	75.3	4	36.1	60.6	87	68.4	17.1	787.20
	2019	0	7.3	12.4	122.1	200	816.6	79.3	49.7	55.2	181.1	204.5	138.7	1866.90
	2020	123.2	22.6	185.4	240.7	127.1	87	37.7	114.8	103.5	139.3	59.7		1241.00
	2021	0	38.4	26	237.7	189.9	24.7				136.3	33.6		686.60

Dara Malo	1992	12.3	35	48.3	83.6	95.5	99.1	77.6	28.4	128.5	61.6	53	18.8	741.70
	1993	19.1	92.2	19.2	135.9	115	91	26.1	55	79.8	86.3	7.2	0	726.80
	1994	1.8	12.7	77.6	177.6	191.2	52.7	71.5	153.9	50.6	69.7	86.2	1	946.50
	1995	0	36.1	67.1	202.9	81	53.3	87.2	59.6	81.1	82.9	54.9	52.7	858.80
	1996	51	15.9	87	224.2	152	120.7	86.8	139.6	137.8	58.5	32.8	4.4	1110.70
	1997	16.7	0	49	198.7	82.4	68.9	115.7	96.2	122	322.4	364.2	66.9	1503.10
	1998	95.7	65.7	102	144.4	149.3	106.1	78.4	46.9	49.1	116.8	15.8	1	971.20
	1999	23.7	0	89.4	106.8	55.3	57	113.4	44.3	68.2	170	2.9	4	735.00
	2000	0	0	12.7	109.6	151.7	98.4	94.3	83.6	68.3	166.3	20.5	3.1	808.50
	2001	13.4	9.5	113.3	206.4	153.6	78.1	31.9	127.3	103.2	150.6	40.8	2.5	1030.60
	2002	25	17.2	169	104.5	114.6	35.6	47	70.3	130.9	77.4	25.3	74.2	891.00
	2003	17.4	37.3	140.8	171	94.2	129.6	84.7	178.9	94.3	54.5	38	8.3	1049.00
	2004	46.4	7.8	64.1	184.3	64.4	29	58	86.9	44.2	47.8	97.4	74.8	805.10
	2005	24.3	5.9	64.3	99.4	291.7	34.2	125.6	80.4	129.5	74.1	46.2	0	975.60
	2006	14.6	35.4	104.7	140.7	84.8	66.3	77.4	121.3	71.3	150.5	93.8	100.4	1061.20
	2007	19.8	19.8	48.4	62.4	174.2	88.5	145.6	94.9	233	85.2	39.2	0	1011.00
	2008	2.5	2	16.3	151	88.8	91.9	30.6	122.1	128	89.2	96.5	4	822.90
	2009	30.7	1.5	47.4	146	93.9	36	20.7	62.6	79.8	112.5	64.1	72.8	768.00
	2010	38.7	34.1	216.6	205.3	174.9	87.7	80.9	120.3	78.6	46.7	10	39.1	1132.90
	2011	1.8	2.4	41.4	40.4	209.3	89.5	140	62.6	119.6	3	0	0	710.00
	2012	38.2	140.1	140.8	91.1	94.8	146.2	192.1	26.2	90.6	13.2	205.8	58	1237.10
	2013	93.1	70.8	167.9	136.9	23.6	0	2.1	59.7	42.6	197.5	227.7	85.3	1107.20
	2014	43	98.8	135.7	263.3	37	1.3	0	0	76.3	152.7	172.5	105.1	1085.70
	2015	114.4	41.4	0	0	17	19.8	138.6	16.3	153.1	236.1	102.3	124.2	963.20
Chancho	2001	12.5	12.9	134.9	39.8	124.5	158.3	332.4	276.8	38.1	0	0	0	1130.20
	2002	38.4	49.4	134	56.1	48.5	315.8	720	499.5	61.5	3.5	0	39.1	1965.80
	2003	57.5	49	79.2	206.9	4.5	315.1	778.3	834.3	581.4	0	3.5	27.9	2937.60
	2004	68.2	0	27.2	79.8	21.7	694.3	1154.8	778.7	360.5	115.6	0	13.4	3314.20
	2005	5.3	71.4	0	38.7	76.6	196.4	263.6	312.6	351.3	1.5	0	0	1317.40
	2006	0	10.4	133.6	104.3	75.7	187.2	394.6	321.2	229.7	3	0	16.2	1475.90
	2007	12.5	46.5	26.1	50.4	105.9	154	325.1	276.7	124.2	14.8	0	0	1136.20
	2008		0	0	44.1	133.8	350	445.6	70.4	0	29	50.6	0	1123.50
	2009	33.5	23.9	39.9	2.3	6.2		491.3	653.4	411.4	86.4	0	62.3	1810.60
	2010	16.2	67.8	57.2	109.6	99.2	294.6	372.5	333.3	271.7	0	3.6	16.7	1642.40
	2011	16	3.3	29	40.4	77.7	114.6	422.3	526.7	304.9	684.6	0	0	2219.50
	2012	0	0	6.9	87.3	47.7	98.3	622.7	565.8	415	0	0	0	1843.70
	2013	0	0	24	86.1	3	264	343.4	273.7	235.4	6.2	5.9	0	1241.70
	2014	2.4	0	64.6	40.9	63	8.3	287.4	600	366.8	1.3	0	0	1434.70

2015	0	0	12.5	7.9	179.2	198	358.8	752.6	55.1	16.7	16.7	9	1606.50
2016	14.1	0	69	172.8	237.6	348.5	619.6		246.7	8.2	18.4	0	1734.90
2017	0	0	1	16.6	84.8	104.4	589.5	450.2	200.1	0	0		1446.60
2018	0	0	31.6	126.4	48.4	160	513.3	407.9	91.9	0	11.3	13.4	1404.20
2019	0	8.3	75	46.2	62	174.8	463.5	301.4	254.9	20.5	6.5	9.1	1422.20
2020	0.7	24			110.2	164.6	461.3	554.6	50.3	21.7	18	6.5	1411.90
2021	0	18	0	50.5	674.5	484.2	67.2	0	0	335	286		1915.40

Appendix II Pair-wise comparison matrix of each causative factors

factor	slope	aspect	curvature	LULC	NDVI	Lithology	Distance-road	Distance-fault	Distance-stream	Distance-lineament
slope	1	3	4	3	3	5	5	8	6	9
aspect	0.333333	1	3	3	4	4	3	5	4	7
curvature	0.25	0.333	1	3	3	5	3	5	7	5
LULC	0.333	0.333	0.333	1	3	3	3	3	3	8
NDVI	0.333	0.25	0.333	0.333	1	3	3	3	3	6
Lithology	0.2	0.25	0.2	0.333	0.333	1	3	3	3	7
Distance-road	0.2	0.333333	0.333333	0.333333	0.333333	0.333333	1	3	3	3
Distance-fault	0.125	0.2	0.2	0.333	0.333	0.333	0.333	1	3	5
Distance-stream	0.166667	0.25	0.142857	0.333333	0.333333	0.333333	0.333333	0.333333	1	3
Distance-lineament	0.111	0.143	0.2	0.125	0.1667	0.142857	0.333333	0.2	0.333333	1
SUM	3.053	6.093	9.743	11.792	15.5	22.143	22	31.53333	33.33333	54

Appendix III Normalized Pair-wise comparison matrix of each causative factors

factor	slope	aspect	curvature	LULC	NDVI	Lithology	Distance-road	Distance-fault	Distance-stream	Distance-lineament	SUM	criteria Weight	Criteria Weight (%)
slope	0.327571	0.49238	0.410557	0.254417	0.193548	0.225806	0.227273	0.2537	0.18	0.166667	2.731919	0.273192	27.31919
aspect	0.10919	0.164127	0.307918	0.254417	0.258065	0.180645	0.136364	0.158562	0.12	0.12963	1.818917	0.181892	18.18917
curvature	0.081893	0.054709	0.102639	0.254417	0.193548	0.225806	0.136364	0.158562	0.21	0.092593	1.510531	0.151053	15.10531
LULC	0.10919	0.054709	0.034213	0.084806	0.193548	0.135484	0.136364	0.095137	0.09	0.148148	1.081599	0.10816	10.81599
NDVI	0.10919	0.041032	0.034213	0.028269	0.064516	0.135484	0.136364	0.095137	0.09	0.111111	0.845316	0.084532	8.453156
Lithology	0.065514	0.041032	0.020528	0.028269	0.021505	0.045161	0.136364	0.095137	0.09	0.12963	0.67314	0.067314	6.731395
Distance-road	0.065514	0.054709	0.034213	0.028269	0.021505	0.015054	0.045455	0.095137	0.09	0.055556	0.505411	0.050541	5.054113
Distance-fault	0.040946	0.032825	0.020528	0.028269	0.021505	0.015054	0.015152	0.031712	0.09	0.092593	0.388584	0.038858	3.885838
Distance-stream	0.054595	0.041032	0.014663	0.028269	0.021505	0.015054	0.015152	0.010571	0.03	0.055556	0.286395	0.02864	2.863951
Distance-lineament	0.036397	0.023447	0.020528	0.010601	0.010753	0.006452	0.015152	0.006342	0.01	0.018519	0.158189	0.015819	1.581888
											10	1	100

Appendix IV Calculated consistency

C.W	0.273192	0.181892	0.151053	0.10816	0.084532	0.067314	0.050541	0.038858	0.02864	0.015819			
factor	slope	aspect	curvature	LULC	NDVI	Lithology	Distance-road	Distance-fault	Distance-stream	Distance-lineament	Weighted sum	C.W	Ratio
slope	0.273192	0.545675	0.604212	0.32448	0.253595	0.33657	0.252706	0.310867	0.171837	0.14237	3.215503	0.273192	11.77013
aspect	0.091064	0.181892	0.453159	0.32448	0.338126	0.269256	0.151623	0.194292	0.114558	0.110732	2.229182	0.181892	12.25555
curvature	0.068298	0.060631	0.151053	0.32448	0.253595	0.33657	0.151623	0.194292	0.200477	0.079094	1.820112	0.151053	12.04948
LULC	0.091064	0.060631	0.050351	0.10816	0.253595	0.201942	0.151623	0.116575	0.085919	0.126551	1.24641	0.10816	11.52377
NDVI	0.091064	0.045473	0.050351	0.036053	0.084532	0.201942	0.151623	0.116575	0.085919	0.094913	0.958445	0.084532	11.33831
Lithology	0.054638	0.045473	0.030211	0.036053	0.028177	0.067314	0.151623	0.116575	0.085919	0.110732	0.726716	0.067314	10.79591
Distance-road	0.054638	0.060631	0.050351	0.036053	0.028177	0.022438	0.050541	0.116575	0.085919	0.047457	0.55278	0.050541	10.93723
Distance-fault	0.034149	0.036378	0.030211	0.036053	0.028177	0.022438	0.016847	0.038858	0.085919	0.079094	0.408125	0.038858	10.50288
Distance-stream	0.045532	0.045473	0.021579	0.036053	0.028177	0.022438	0.016847	0.012953	0.02864	0.047457	0.305148	0.02864	10.6548
Distance-lineament	0.030355	0.025985	0.030211	0.01352	0.014089	0.009616	0.016847	0.007772	0.009547	0.015819	0.173759	0.015819	10.98427
													11.28123

Where, λmax is 11.28123 and RI is 1.49